WORLD SMALL ANIMAL VETERINARY ASSOCIATION RENAL PATHOLOGY INITIATIVE: CLASSIFICATION OF GLOMERULAR DISEASES IN DOGS

R.E. Cianciolo[1], F.C. Mohr[2], L. Aresu[3], C.A. Brown[4], C. James[5], J.H. Jansen[6], W.L. Spangler[7], J.J. van der Lugt[8, 18], P.H. Kass[9], C. Brovida[10], L.D. Cowgill[11], R. Heiene[12-14], D.J. Polzin[15], H. Syme[16], S.L. Vaden[17] A.M. van Dongen[18], and G.E. Lees[19]

[1]Department of Veterinary Biosciences, College of Veterinary Medicine, The Ohio State University, Columbus OH

[2]Department of Pathology, Microbiology and Immunology, School of Veterinary Medicine, University of California, Davis, CA

[3]Facoltà di Medicina Veterinaria, Dipartimento di Biomedicina comparata e Alimentazione, Università di Padova, Legnaro, Italy

[4]Athens Veterinary Diagnostic Laboratory, College of Veterinary Medicine, University of Georgia, Athens GA

[5]IDEXX Laboratories, Ltd., Wetherby, United Kingdom

[6]Department of Basic Sciences and Aquatic Medicine, Norwegian University of Life Sciences, Oslo, Norway

[7]NSG Pathology, Davis, CA

[8] IDEXX Europe, B.V., Hoofddorp, The Netherlands

[9]Department of Population Health and Production, School of Veterinary Medicine, University of California, Davis, CA

[10]ANUBI Ospedale per Animali da Compagnia, Moncalieri, Italy

[11]Department of Medicine and Epidemiology, School of Veterinary Medicine, University

of California, Davis, Davis, CA

[12]Blue Star Animal Hospital, Gothenburg, Sweden

[13]PetVett Dyresykehus, Oslo, Norway

[14]Department of Companion Animal Clinical Sciences, Norwegian University of Life Sciences, Oslo, Norway

[15]Department of Veterinary Clinical Sciences, College of Veterinary Medicine, University of Minnesota, St Paul, MN

[16]Department of Clinical Sciences, Royal Veterinary College, Hatfield, UK

[17]Department of Clinical Sciences, College of Veterinary Medicine, North Carolina State University, Raleigh, NC

[18]Department of Clinical Sciences of Companion Animals, Faculty of Veterinary Medicine, Utrecht University, Utrecht, The Netherlands

[19]Department of Small Animal Clinical Sciences, College of Veterinary Medicine and Biomedical Sciences, Texas A&M University, College Station, TX

Acknowledgements:

This work was performed under the auspices of the World Small Animal Veterinary Association Standardization Projects program with generous financial support from Hill's Pet Nutrition and from Bayer Animal Health.

The authors acknowledge the substantive contributions of Dr. Brian R. Berridge (Glaxo Smith Kline, Raleigh, NC) and Dr. Fred J. Clubb, Jr. (Department of Veterinary Pathobiology, Texas A&M University, College Station, TX) to the conceptualization and initial planning of this project. Additionally, the authors gratefully thank Ralph Nichols

(Texas Heart Institute, Houston, TX) and Mary Sanders (Department of Small Animal Clinical Sciences, Texas A&M University, College Station, TX), the staff of the Department of Pathobiology at Utrecht University, and the staff at the University of Padova for their expert technical assistance, without which this project could not have been completed.

ABSTRACT

Evaluation of canine renal biopsy tissue has generally relied on light microscopic (LM) evaluation of hematoxylin and eosin-stained sections ranging in thickness from 3 to 5µm. Advanced modalities, such as transmission electron microscopy (TEM) and immunofluorescence (IF), have been used sporadically or retrospectively. Diagnostic algorithms of glomerular diseases have been extrapolated from the World Health Organization classification scheme for human glomerular disease. With the recent establishment of two veterinary nephropathology services, which evaluate 3 µm sections with a panel of histochemical stains and routinely perform TEM and IF, a standardized objective species-specific approach for the diagnosis of canine glomerular disease was needed. Eight veterinary pathologists evaluated 114 parameters (lesions) in renal biopsy specimens from 89 dogs. Hierarchical cluster analysis of the data revealed two large categories of glomerular disease, based on the presence or absence of immune complex deposition. The immune complex-mediated glomerulonephritis category included cases with a membranoproliferative or membranous pattern on histology. Non-immune complex mediated glomerulonephropathies included control dogs and dogs with glomerular amyloidosis or focal segmental glomerulosclerosis. Cluster analysis performed on only the LM parameters led to misdiagnosis of 22 of the 89 cases, *i.e.,* ICGN cases moved to the non-ICGN branch of the dendrogram or vice versa, emphasizing the importance of advanced diagnostic modalities in the evaluation of canine glomerular disease. Salient LM, TEM and IF features for each pattern of disease were identified, and a preliminary investigation of related clinicopathologic data was performed.

INTRODUCTION

Diagnosis of canine glomerular disease has been based, in part, on the World Health Organization (WHO) classification system created to define and standardize the categories of human glomerular disease.[10,12,16,17,20,22,24,27,31-33,38,42,44,49,50,52,54] Although human glomerular disease is routinely defined following (1) examination of thin (3 μm) light microscopic (LM) sections viewed with a specific panel of histochemical stains, (2) immunofluorescence (IF) to detect the presence of immunoglobulins and complement components, and (3) transmission electron microscopy (TEM), this has generally not been the case with diagnosis and classification of glomerular disease in dogs.[10,12,20,24,32,33,38,44,50,54] Moreover, it is apparent that although canine glomerular diseases share many of the structural characteristics seen in their human counterparts, there are striking differences as well. The infrequent use of advanced diagnostic modalities and the uncertainty regarding the accuracy of a diagnosis based solely on histopathology has created concerns regarding the clinical utility of canine renal biopsy. Furthermore, the dearth of peer-reviewed literature examining epidemiological, therapeutic and outcome factors in dogs with spontaneous glomerular disease can be partly explained by the non-standardized, often retrospective, analysis of renal tissue by veterinary pathologists.

To address these concerns, the World Small Animal Veterinary Association-Renal Standardization Study Group (WSAVA-RSSG) was conceived at Netherland's Utrecht University in January 2005.[13,25] This international group of veterinary nephrologists and pathologists set out to design a study that would develop a comprehensive understanding

of glomerular disease in dogs by routinely using standardized LM, IF, and TEM methods to evaluate renal biopsies and by associating the pathologic findings with detailed clinical and case outcome data. Two veterinary diagnostic renal pathology centers, one in the U.S.A. and one in Europe, were established to perform the evaluations and facilitate the collection of cases for prospective studies. The U.S.A. center, created in 2005 at Texas A&M University as the Texas Veterinary Renal Pathology Service (TVRPS), was reorganized in 2013 as the International Veterinary Renal Pathology Service (IVRPS) and now operates as a joint effort between The Ohio State University and Texas A&M University. The Utrecht Veterinary Nephropathology Service (UVNS) began examining renal biopsies at Utrecht University, Netherlands, in 2008. The UVNS currently works in cooperation with the Department of Comparative Biomedicine and Food Science at the University of Padova, Italy. The IVRPS and UVNS demonstrated that canine renal biopsies could be evaluated with LM, IF and TEM in a reasonable diagnostic workflow to provide timely and useful information to clinicians.[11]

The goals of this study are 1) Development of a digital pathology platform to allow WSAVA-RSSG pathologists in widely dispersed geographic locations to communicate and collaborate effectively. Using that platform, digitized LM slides, IF and TEM images can be remotely accessed and evaluated by individuals and by the group during online meetings. 2) Development of succinct definitions and scoring criteria for glomerular, tubular, interstitial and vascular lesions. 3) Use of hierarchical cluster analysis to objectively identify common patterns of glomerular injury in dogs in order to create a simplified, reproducible, and accurate guide for veterinary pathologists to use when evaluating renal biopsies from dogs with proteinuric renal disease.

MATERIALS AND METHODS

Case Selection

Dogs in this study had renal biopsies performed because they exhibited proteinuria indicative of the presence of glomerular disease, *i.e.,* persistent renal proteinuria with urine protein to creatinine rations (UPC) values ≥2.0, which was subsequently confirmed by biopsy findings.[23] Additionally, a case had to have biopsy specimens sufficient for diagnosis, *i.e*., either LM, TEM, and IF findings, or LM and TEM findings without IF findings if the LM and TEM findings alone were conclusive. Lastly, five dogs without clinicopathologic indications of renal disease were chosen from the TVRPS database to serve as controls. These dogs were racing Greyhounds from which renal biopsies were performed during ovariohysterectomy prior to adoption as pets.[45]

Clinical Data

Dogs with glomerular disease exhibited a diverse spectrum of clinical illnesses that had been evaluated and treated in various ways before their renal biopsies were obtained. Detailed analysis of the clinicopathologic features of the illnesses exhibited by the dogs was beyond this study's scope, which was focused on developing a prototype method for classification of canine glomerular diseases based on pathologic features. Nevertheless, several key clinical laboratory findings provided by submitting veterinarians were compiled for each dog. These findings included: magnitude of proteinuria, (defined as the highest UPC value observed before biopsy), serum creatinine concentration (defined as the last value observed before biopsy), and serum albumin concentration (defined as the lowest value observed before biopsy). Also, the presence or

absence of hypertension, defined as a recorded systolic value consistently > 160 mmHg before biopsy or if the dog was being treated with any antihypertensive medication (other than an ACE-inhibitor drug alone) at the time of biopsy, was evaluated with the clinical laboratory data.

Light Microscopy

All specimens for LM evaluation were immersion-fixed in 10% buffered formalin, processed and embedded in paraffin. Tissues were serially sectioned at least ten times at 3 μm thickness and stained with hematoxylin and eosin (HE), periodic acid Schiff's reagent (PAS), Masson's trichrome (TRI), and the Jones methenamine silver method (JMS). Additionally, thicker (8μm) sections were cut from at least one cortical specimen and stained with Congo red (CR). All histochemical procedures were performed using established methods.

Transmission Electron Microscopy

Transmission electron microscopy was performed at Texas Heart Institute (Houston, TX) and at Department of Comparative Biomedicine and Food Science, University of Padova using similar techniques. Briefly, renal tissue containing glomeruli was fixed in chilled 3% phosphate buffered glutaraldehyde. Specimens were post-fixed in 1% osmium tetroxide, serially dehydrated, infiltrated in an acetone/epoxy plastic, and embedded in plastic. In one dog, glomeruli were not present in the glutaraldehyde-fixed sample. For that case, the paraffin embedded tissue from the LM specimen was harvested and postfixed in 1% osmium tetroxide and embedded in EM BED 812 and Araldite (Electron Microscopy Sciences, Fort Washington, PA, USA). Plastic blocks were cut with a Sorvall MT2-B ultramicrotome. Thick sections (1 μm) were stained with toluidine

185 blue. These sections were evaluated and appropriate areas were identified for thin
186 sectioning. Thin sections were cut at silver-grey interference color (55-60 nm) and placed
187 on copper mesh grids. Grids were stained with uranyl acetate and lead citrate and were
188 examined with a JEOL-TEM-1230 transmission electron microscope and digital
189 photomicrographs were obtained.
190 *Immunofluorescence*
191 Tissues were immersed in chilled Michel's Transport Medium (Newcomer
192 Supply, Middleton, WI, USA) for up to 72 hours during transport to the pathology
193 laboratory where they were washed 3 times in Michel's Wash (Newcomer Supply,
194 Middleton, WI, USA), placed in plastic cryomolds filled with Tissue-Tek OCT
195 embedding compound (Electron Microscopy Sciences, Fort Washington, PA, USA), and
196 snap-frozen in liquid nitrogen. Blocks were stored at -80^{o}C until sectioned. Thin (4μm)
197 cryosections were cut on a Leica CM 1850 UV cryostat (Bannockburn, IL, USA) and
198 stored at -80^{o}C until thawed for one hour at room temperature for staining. Sections were
199 fixed for five minutes in cold 100% acetone, air dried for one hour, then rehydrated in
200 phosphate-buffered saline. Direct IF was performed with fluorescein isothiocyanate-
201 (FITC)-conjugated polyclonal goat anti-dog IgG, IgM, IgA, and C3 antibodies (Bethyl
202 Labs, Montgomery, TX, USA), as well as with FITC-conjugated polyclonal rabbit anti-
203 human C1q, kappa light chain, and lambda light chain antibodies (Dako North America,
204 Carpinteria, CA, USA). Sections were incubated for one hour with an appropriate
205 dilution of each antibody, then washed with phosphate-buffered saline. Sections were
206 coverslipped using a mounting medium that retarded fluorescence quenching (Prolong
207 Gold, Invitrogen, Carlsbad, CA, USA), and were examined using appropriate filters with

208 an epifluorescence microscope (Olympus, Center Valley, PA, USA).

209 *Image acquisition and viewing*

210 Renal biopsies prepared for LM were digitally scanned with a slide scanning
211 instrument.[a] Scanned slides along with digitized TEM and IF images were stored and
212 managed by digital pathology software[b] for review,[c,d] both by individual pathologists and
213 during group conferences.[e] Specifically, digital images from all three modalities were
214 reviewed and graded independently by all eight pathologists prior to group discussions.

215 *Scoring*

216 For each of the three methods of examination, changes in the renal tissue were
217 deconstructed to their most basic components, which were then discussed by the
218 pathologists to formulate the most appropriate way to assess each lesion. Some lesions
219 were scored as present or absent, whereas others were given a severity grade. These
220 discussions also facilitated the clarification of descriptive terms for the various lesions
221 (Supplement Table 1). This process produced the LM, TEM, and IF scoring schemes
222 described below. Pathologists filled out an electronic evaluation form for each case.
223 Scores were collated by a single pathologist (REC), and either averages or consensus
224 scores were used for data analysis, as discussed below.

225 LM: The histologic features evaluated are listed in Table 1a. Two different
226 grading schemes were required in order to assess distribution and severity of features.
227 One set of lesions was scored based on whole slide evaluations of glomerular, interstitial,
228 and vascular compartments. These lesions were scored on a scale of 0-4 representing
229 different degrees of intensity including: not present, present but rare, mild, moderate, and
230 severe, respectively. In instances of general agreement on the survey, the average score

was used for statistical analysis; however, consensus scores (based upon discussions during online conferencing sessions) were used for the occasional instances in which survey responses varied widely. The second set of lesions was scored by evaluating individual glomeruli (4 to 32 glomeruli per case) and individual fields of tubulointerstitium, measuring 400 x 600µm (5 to 32 fields per case) to detect focal lesions. Each pathologist graded a set of unique glomeruli and tubulointerstitial fields. Scores were reported as percent of glomeruli (or tubulointerstitial fields) affected for statistical analysis. The percent of glomeruli affected would determine focal versus diffuse disease processes but not necessarily segmental versus global glomerular lesions.

TEM: The digital TEM images from each case (9-26 images per case) were viewed and scored independently by the pathologists. The specific location of any glomerular electron-dense deposits and the remodeling of the glomerular basement membrane (GBM) (as listed in Table 1b) were scored as absent (0), rare (1) or not rare (2). Additional TEM lesions were scored as absent (0) or present (1).

IF: Diagnostic evaluation of IF labeling patterns (Table 1b) were performed by GL and JvdL, and representative digital photographs of one to three glomeruli with notable labeling with each antibody were taken at that time. All pathologists evaluated the IF images for each case prior to group discussions, and by consensus agreement, the scores used in the data analysis for the IgG, IgM, IgA, and C3 immunostains were those provided by the pathologist (REC), who had extensive training and experience evaluating glomerular IF labeling patterns. Specifically, a score of 2 was given when there was consistent granular labeling in the mesangium or capillary walls above the background autofluorescence of the tubulointerstitial compartment. A stain was deemed equivocal

and given a score of 1 when there were a few scattered granules or labeling of low intensity in the glomeruli. Non-specific labeling patterns (eg, not granular) and the absence of positive labeling were scored as 0.

Statistical Analysis

Hierarchical cluster analysis was used to organize the cases into groups. Within each group (cluster), cases had greater similarity to each other (in terms of the evaluated lesions) than they did to cases from other groups. Cluster analysis, therefore, objectively organized the cases into distinct groups of dogs having similar pathologic changes (patterns of injury). The procedure used for this analysis was Ward's linkage with L2 dissimilarity[f]. Results of each analysis were displayed as a dendrogram in which the shorter the vertical lines under the horizontal bar connecting two animals (or groups of animals), the lesser the dissimilarity among shared parameters.

Cluster analysis was performed on three datasets containing the same number of cases but differing in the number of lesions (parameters) evaluated. The first dataset contained all 114 parameters (LM: 76, TEM: 30, IF: 8). The second, which had 59 parameters (LM: 35, TEM: 16, IF: 8), was a limited list selected by the pathologists, based on their expertise gained during the course of the study. This limited list excluded parameters that were rarely observed or deemed to be uninformative. Lastly, the third dendrogram was generated from the 59-parameter dataset using only LM lesions (35 parameters).

Some of the categorical values for IF were missing because the biopsy tissue apportioned for IF did not contain glomeruli for some or all of the immunostains. This included cases of glomerular amyloidosis (5 cases), membranous glomerulonephropathy

(3 cases) and glomerulosclerosis (1 case). Because cluster analysis cannot be performed on data sets with missing values, a method was developed to add imputed values for the missing data. Ordinal logistic regression was used to predict the probability of an individual with missing data falling into one of the three possible mutually exclusive categories (0, 1, 2) as a function of other variables believed *a priori* to be associated with IF. The category with the highest predicted probability was assigned for each individual's missing IF value.

Using the 59-parameter dataset, Mann-Whitney tests were performed with the same software to determine if significant differences existed for the parameters within clusters exhibiting similar glomerular disease patterns (Clusters 2 *vs*. Cluster 3, Cluster 5 *vs*. Cluster 6 and Cluster 7 *vs.* Cluster 8).

RESULTS

Cluster Analysis

Ninety-six dogs (including the five controls) were scored, and a preliminary cluster analysis was performed (data not shown). This preliminary cohort contained seven cases with rare diagnoses, including one collagenofibrotic glomerulonephropathy (based on the presence of type III collagen within the capillary wall and mesangium), one canine Alport syndrome (based on the lack of normal Type IV collagen in the GBM), two non-amyloidotic fibrillary glomerulonephropathies, one podocytopathy, and two cases with GBM defects of undetermined pathogenesis. Given that these cases obscured the findings of the patterns of the larger clusters, the decision was made to remove them from the cohort so that the study could focus on the patterns of common types of canine glomerular disease. Exclusion of these seven cases resulted in a cohort of five controls

300 (from the TVRPS center) and 84 proteinuric dogs (73 from the TVRPS center and 11
301 from the UVNS center). Fifty-nine cases had been prospectively enrolled through the
302 WSAVA-sponsored study, and the remaining cases had routine diagnostic samples that
303 met the aforementioned criteria. Needle core biopsies were performed in 72 dogs; 16
304 dogs had surgical wedge biopsies; one dog had a surgical punch biopsy.
305 The dendrogram generated from the 114-parameter set is shown in Fig.1. There
306 were two large branches. The cases on the right (n=46) were defined by the presence of
307 electron-dense (immune complex) deposits and were considered to have immune
308 complex-mediated glomerulonephropathies (ICGN), whereas cases on the left (n= 43,
309 including the five controls) did not typically have immune deposits and were considered
310 to be non-ICGN. Of note, there were 6 cases in the non-ICGN branch with equivocal
311 evidence that immune complexes might have played a role in the evolution of their
312 glomerular disease; however, the dominant phenotype at the time of biopsy was that of
313 glomerulosclerosis. These exceptions are discussed below in the glomerulosclerosis
314 section. The two large branches disaggregated into progressively smaller groups and
315 eventually partitioned into eight distinct clusters. Cluster 1 was composed of the five
316 control animals with normal glomerular morphology, clinical findings and laboratory
317 values. Clusters 2 and 3 were comprised of cases with glomerulosclerosis. Interestingly,
318 cases in Cluster 2 shared more similarities to controls in Cluster 1 than to cases in Cluster
319 3, as demonstrated by the presence of a connecting link between Clusters 1 and 2. Cluster
320 4 was comprised of cases of glomerular amyloidosis. Cases in Clusters 5 and 6 and
321 Clusters 7 and 8 had patterns that were characteristic of membranoproliferative
322 glomerulonephritis (MPGN) and membranous glomerulonephropathy (MGN),

323 respectively.

324 A dendrogram of the 59-parameter dataset was also generated (Fig. 2). Similar to
325 the 114-parameter dataset, this dendrogram clearly showed a division of cases into 8
326 distinct clusters. With one exception, the case composition of each cluster was identical
327 to the case composition of the clusters formed from the larger, 114-parameter dataset.
328 However, the ordering of cases and the formation of smaller subclusters differed between
329 the two dendrograms, and one case moved from Cluster 6 to Cluster 7, representing a
330 shift from a MPGN pattern to a MGN pattern.

331 Often the only modality routinely available for evaluation of renal tissue is LM;
332 therefore cluster analysis was also performed on only the LM lesions (31 parameters)
333 from the 59-parameter dataset (Fig. 3). This enabled comparison of the LM-only
334 dendrogram to Fig. 2. While Fig. 3 also contained eight clusters, it failed to correctly
335 distinguish a number of ICGN cases from non-ICGN cases. Specifically, eight of the
336 MGN cases (seven of 10 cases in Cluster 8 and one of 14 cases in Cluster 7), all of which
337 had unequivocal evidence of immune deposits demonstrated with TEM and IF, moved to
338 the non-ICGN side of the dendrogram. In addition, all 13 cases in Cluster 3 and one of 13
339 cases in Cluster 2 (glomerulosclerosis clusters) moved to the ICGN side of the
340 dendrogram. This demonstrates that evaluating renal biopsies solely by LM can introduce
341 significant errors that would have adverse therapeutic and prognostic implications.
342 Moreover, it clearly illustrates the importance of TEM and IF for the correct
343 classification of canine glomerular disorders.

344 ***Control kidneys***

345 Five controls had glomeruli with minimal lesions *via* all analyses of renal biopsies

and were considered normal (Cluster 1). All five dogs were initially enrolled into the study as controls because they lacked proteinuria and azotemia. Most glomeruli were histologically normal. Specifically, glomerular tufts were usually normocellular, capillary walls were thin and the mesangium was not expanded (Figs. 4-7). Fuchsinophilic deposits were not observed (Fig. 6). Minimal histologic lesions were identified in a few glomeruli from each biopsy, including mild segmental mesangial cell hypercellularity (3 or more mesangial cell nuclei in close apposition) and mild mesangial expansion. Notably, segmental glomerulosclerosis was not present (Tables 2 and 3). Small synechiae and GBM hyalinosis were rarely observed (Table 2).

Ultrastructurally, podocyte foot processes were largely intact and the GBM was uniform and homogeneous (Fig. 8). Electron-dense deposits or fibrils were not present (Tables 4 and 5). Cellular interpositioning, GBM rarefaction, and GBM wrinkling were rarely observed in control dogs. Immunofluorescence revealed unequivocal granular IgM labeling in the mesangium in two cases (Fig. 9); one of these cases also had IgM labeling within the capillary walls. Unequivocal labeling for other immunoreactants was not identified in the mesangium or capillary walls (Table 6). Because electron-dense deposits were not identified ultrastructurally, the IgM labeling was considered nonspecific.

Control dogs were not proteinuric, azotemic, or hypoalbuminemic (Table 7). However, four of the five dogs had systolic blood pressures (SBP) between 160 and 180 mmHg and the fifth dog had a SBP of 146 mmHg. The greyhound breed has been reported to have higher blood pressure than other breeds; this elevation in SBP has been attributed to the white-coat effect.[28] Interestingly, the dog with the highest SBP (176mmHg) had the highest percentage of glomeruli with synechiae and hyalinosis (data

not shown).

Focal Segmental Glomerulosclerosis

Twenty-six of 89 cases grouped into two clusters, with 13 cases in Cluster 2 and 13 cases in Cluster 3; all had lesions characteristic of the pattern of focal segmental glomerulosclerosis (FSGS). The defining light microscopic lesion of these clusters was solidification of a portion of the capillary tuft in at least one glomerulus. This segmental solidification was attributed to mesangial matrix expansion and effacement of the capillary lumen, often in association with some degree of mesangial hypercellularity (Figs. 10-13). The distribution of the sclerosis within the glomerular tuft (hilar, near the origin of the proximal tubule, or not at the poles) was highly variable among the glomeruli even within a single biopsy core. Glomerulosclerosis was more severe and affected more glomeruli in Cluster 3 compared with Cluster 2 (Tables 2 and 3). Specifically, the percent of non-obsolescent glomeruli affected by FSGS ranged from 3 to 100%, with a significantly higher percentage of affected glomeruli in Cluster 3 compared with Cluster 2. Synechiae and hyalinosis of the tuft were commonly observed lesions in FSGS and were likewise more extensive in Cluster 3 compared with Cluster 2 (Tables 2 and 3). A significantly higher percentage of glomeruli in Cluster 3 had synechiae, mesangial matrix expansion, nuclear debris and periglomerular inflammation compared with glomeruli in Cluster 2. In 19 of the 26 cases comprising Clusters 2 and 3, obsolescent glomeruli were present, involving 0 to 43% of the total number of glomeruli in the biopsies. Obsolescent glomeruli were significantly more prevalent in Cluster 3 than in Cluster 2. Although not tested for significance, the mean percentage of obsolescent glomeruli in Cluster 3 was 22%, whereas it ranged from 0 to 8% in the other clusters.

392 Capillary wall thickening was often mild in Cluster 2, but mild to moderate in Cluster 3
393 (Table 2). Seven of 13 cases in Cluster 3 and one of 13 cases in Cluster 2 had rare
394 changes in the GBM interpreted via LM to be spike or hole formation; however, none of
395 these cases had evidence of GBM spikes or holes ultrastructurally. Three of 26 cases in
396 Clusters 2 and 3 (12%) exhibited segmental distortion of glomerular tufts due to the
397 presence of lipid-laden macrophages (glomerular lipidosis). This lesion was not present
398 in control dogs or in any other disease category in this study.
399 The percentages of tubulointerstitial fields with fibrosis and the severity of the
400 fibrosis were not significantly different between Clusters 2 and 3. The percentages of
401 fields affected by inflammation and the severity of inflammation were significantly
402 greater in Cluster 3 compared with Cluster 2.
403 Although TEM (Fig. 14) revealed extensive foot process effacement in FSGS, this
404 lesion was not specific for Clusters 2 and 3, because it was identified in all proteinuric
405 dogs. Common ultrastructural lesions included: wrinkling of the GBM, GBM rarefaction,
406 mesangial cell interpositioning, microvillus transformation of podocytes, and (in Cluster
407 3) diffuse GBM thickening (Table 5). Electron-dense deposits were not present in 19
408 cases. However, four cases from Cluster 2 and two cases from Cluster 3 contained
409 mesangial electron-dense deposits by TEM. Two of these cases also had subendothelial
410 electron-dense deposits, which were rare in one case and not rare in the other. One
411 additional case had rare intramembranous electron-dense deposits only. Other TEM and
412 LM lesions in these 7 cases with demonstrable electron-dense deposits were similar to
413 those present in FSGS cases without deposits.
414 Immunofluorescence (Fig. 15) revealed positive capillary wall and/or mesangial

415 labeling of varying intensity for various immunoreactants in many of the FSGS cases and
416 did not distinguish between cases with or without electron-dense deposits. Of the 19
417 FSGS cases without electron-dense deposits present ultrastructurally, 11 had positive
418 unequivocal IF labeling. Of the seven cases with electron-dense deposits noted on TEM,
419 four had granular IgM mesangial staining. One of these four also had granular IgG
420 staining along capillary walls, whereas another had granular C3 staining within the
421 mesangium and along capillary walls.

422 As a group, dogs in Cluster 3 had slightly higher median UPC and SCr values and
423 a greater frequency of hypertension than dogs in Cluster 2 (Table 7), suggesting a trend
424 toward more severe clinical manifestations of disease for dogs in Cluster 3 compared
425 with those in Cluster 2. However, the differences were small and the variation among
426 dogs in each cluster was large, therefore statistically significant differences were not
427 identified.

428 ***Amyloid***

429 Twelve of 89 cases clustered into one group (Cluster 4), and all were diagnosed
430 with glomerular amyloidosis. The defining LM feature of this cluster was expansion of
431 the mesangium and compression of peripheral capillary loops by Congophilic material
432 that was birefringent under polarized light. Amyloid was present as scattered small
433 nodules in three of the cases and as larger, easily discernible, coalescing to occasionally
434 global deposits in the remaining cases (Fig.16-21). Amyloid was pink and waxy when
435 stained with PAS, mottled blue to orange with TRI and did not take up silver with the
436 JMS method. Endocapillary hypercellularity was not present in any case. When present,
437 mesangial hypercellularity was mild. Small synechiae were present in all cases, and in

438 one case involved all glomeruli. Interstitial changes were variable and mild, consisting of
439 interstitial edema, interstitial amyloid, and amyloid deposition within vessel walls. Small
440 amounts of interstitial amyloid were observed in seven of the 12 cases, four of which also
441 had rare vascular amyloid deposits. An additional two cases had vascular amyloid
442 without detectable interstitial deposits.
443 Ultrastructurally, all cases had amyloid deposition characterized by the presence
444 of non-branching 8-15 nm diameter fibrils within the mesangium and capillary wall
445 predominantly in subendothelial and mesangial locations (Figs. 22-23). Foot process
446 effacement was a consistent finding. Electron-dense deposits were not present
447 ultrastructurally. Immunofluorescence labeling revealed occasional equivocal labeling
448 with all immunoreactants (Table 6).
449 As a group, dogs with amyloidosis did not have categorically higher UPC or SCr
450 values or lower SAlb values than other clusters (Table 7). Median UPC values from
451 Clusters 2, 3, 6 and 7 were lower than the median value from dogs with amyloidosis,
452 whereas the median UPC values of Clusters 5 and 8 were higher. Furthermore, three
453 clusters of dogs had higher median SCr values and four clusters of dogs had lower
454 median SAlb values than dogs with amyloidosis. Of note, however, dogs with
455 amyloidosis were hypertensive less frequently than the dogs in any other cluster.
456 ***Immune complex mediated diseases***
457 ***Membranoproliferative Glomerulonephritis***
458 Twenty-three of the 89 cases grouped into two clusters and had a glomerular
459 pattern characteristic of MPGN. Ten cases clustered as one group (Cluster 5) and 13
460 cases clustered as another group (Cluster 6).

By LM, the cases in Cluster 5 and Cluster 6 shared many similar features that were also greater in severity or prevalence than in other clusters. The defining LM feature of MPGN was glomerular hypercellularity that was both endocapillary and mesangial with a global and diffuse distribution (Figs. 24-27). Neutrophils were present within some glomerular capillary loops in all but one case; specifically, they were present in up to 91% of examined glomeruli. This lesion was more frequent in Clusters 5 and 6 compared with other clusters. Glomerular basement membrane duplication (Figs. 25 and 27), highlighted by PAS stains and the JMS method, was prominent in Clusters 5 and 6 and contributed to the observed capillary wall thickening. Nuclear debris, which was scattered in the expanded mesangial matrix, was another prominent characteristic of Clusters 5 and 6. Other LM features shown to be more prevalent in Clusters 5 and 6 were parietal cell hypertrophy and tubular regeneration. Cluster 5 had LM parameters that were greater in intensity or prevalence than those in Cluster 6 including synechiae, GBM hyalinosis, afferent and efferent arteriolar hyalinosis, parietal cell proliferation, splitting of Bowman's capsule and periglomerular fibrosis (Tables 2 and 3). Two tubulointerstitial parameters were more common in Cluster 5 than in Cluster 6: interstitial fibrosis and inflammation.

The major ultrastructural features that distinguished Clusters 5 and 6 from other clusters were the presence of prominent subendothelial and mesangial electron-dense deposits in 23 of 23 cases and 20 of 23 cases, respectively (Fig 28). Other TEM features commonly identified in Clusters 5 and 6 were mesangial cell interpositioning and endothelial cell swelling with lumen effacement. Prominent subepithelial electron-dense deposits were present in one of 10 cases in Cluster 5 and eight of 13 cases in Cluster 6.

These subepithelial deposits were often associated with GBM remodeling. Seven cases in Cluster 6 had ultrastructural evidence of GBM spikes and encircled deposits, while three cases in Cluster 5 had evidence of encircled deposits with no observable GBM spikes. As these cases with subepithelial electron-dense deposits shared the defining light microscopic lesions and prominent subendothelial deposits of MPGN, they were considered a variant of MPGN ("mixed MPGN").

While unequivocal positive labeling for IgA was not observed in any cases in Clusters 5 and 6, clear positive labeling was observed in the capillary wall and/or mesangium for IgG, IgM, and /or C3 in all cases (Fig. 29). There were no significant differences in the IF patterns of all immunoglobulins and C3 between the two clusters.

As a group, dogs in Cluster 5 had somewhat higher median UPC and SCr values and lower median SAlb values than dogs in Cluster 6 (Table 7). These observations suggested a trend toward more severe clinical manifestations of disease for dogs in Cluster 5 compared with those in Cluster 6. However, the ranges of observed values for these variables among dogs in both clusters overlapped so much that it was impossible to discriminate dogs in these two clusters from one another based on these clinical observations. Of note, hypertension was very frequent in these groups; hypertension was more frequent among dogs in Clusters 5 and 6 than among the dogs in any other cluster.

Membranous Glomerulonephropathy

Twenty-three of the 89 cases grouped into Clusters 7 (13 cases) and 8 (10 cases) and had a glomerular pattern characteristic of MGN. Endocapillary hypercellularity was absent to minimal, except for one case in which it was scored as moderate. This parameter did not distinguish MGN clusters from non-ICGN clusters, but clearly

distinguished the MGN pattern from the MPGN pattern (Table 2). Mesangial hypercellularity was minimal to mild in most MGN cases, wherein 3 to 5 mesangial cells per segment were commonly seen in 20 of 23 cases. By LM, most cases of MGN were associated with remodeling of the GBM, consisting of spikes radiating outward from the abluminal surface and/or holes within a thickened GBM (Figs. 30-33). Remodeling was more frequent and more prominent in Cluster 7 compared with Cluster 8. Red nodular deposits, suggestive of immune complexes, visible on the TRI stain were observed via LM in 22 of 23 cases (Fig. 32); however, the deposits were scored as rare in five of these 22 cases. Red nodular deposits observable via LM were more prominent in the MGN pattern compared with the MPGN pattern. Importantly, capillary wall thickening was not specific for the MGN pattern as this feature was also present in other clusters. Significant differences in lesions were noted between Clusters 7 and 8 (Table 2 and 3). Cases in Cluster 7 had more severe GBM remodeling associated with subepithelial immune deposits than did cases in Cluster 8, suggesting that Cluster 7 was associated with more chronic or severe disease. Both synechiae and secondary segmental glomerulosclerosis were significantly more common and / or more severe in Cluster 7 compared with Cluster 8. Hyalinosis of the GBM was mild in Cluster 7 and minimal in Cluster 8. Although these latter parameters were helpful in delineating Cluster 7 from Cluster 8, they were also very prominent features of the FSGS and MPGN patterns (Table 2). Interstitial fibrosis was more common in Cluster 7 compared with Cluster 8. Generally, tubulointerstitial lesions did not differentiate the MGN pattern from other patterns, except for tubular epithelial cell isometric vacuolation, which was more frequent in Cluster 8, compared with all other clusters.

The defining feature of the MGN pattern was the presence of predominantly subepithelial electron-dense deposits on TEM. Electron-dense deposits or GBM changes induced by deposits were usually regularly spaced along the abluminal surface of at least one capillary loop in 22 of 23 cases, whereas the last case had ultrastructural evidence of dissolution of the deposits with only rare electron-dense deposits remaining. Although all MGN cases had subepithelial deposits observed ultrastucturally, red nodular deposits (TRI) were rare or absent via LM in six of these cases. Ultrastructural evidence of GBM remodeling (Fig. 34) was observed in 22 of 23 cases. In addition to prominent subepithelial deposits and GBM remodeling on TEM, seven of the 23 cases also had subendothelial deposits. Despite the presence of subendothelial deposits, the absent to minimal endocapillary hypercellularity observed *via* LM in all but one MGN case separated them from the MPGN pattern. These cases were considered to be a variant of the membranous pattern "mixed MGN".

Immunofluorescence (Fig. 35) revealed unequivocal granular staining patterns for IgG, IgM and C3 within the mesangium and along the GBM in all cases. Similar IF staining patterns were present in cases of the MPGN pattern and could not be used to differentiate between these two classes of immune complex mediated glomerulonephritides.

As a group, dogs in Cluster 8 had somewhat higher median UPC values and were more frequently hypertensive than those in Cluster 7; however, the median SCr and SAlb values for dogs in these 2 clusters were similar (Table 7).

Clinical Observations

Detailed analyses of clinical and laboratory parameters associated with the

553 various patterns of canine glomerular injury included in this study was beyond the scope
554 of this investigation. Nonetheless, key clinical variables were examined to provide a
555 starting point for ongoing and future research that will include a larger number of
556 affected dogs. Several potentially useful observations, which will require verification and
557 further study to define their clinical utility, were made. One was that the magnitude of
558 proteinuria, *i.e.,* UPC values, did not discriminate between different clusters of affected
559 dogs from one another (Table 7). Second, dogs with the MPGN pattern of injury
560 (Clusters 5 and 6) had the most severe constellation of associated clinical abnormalities:
561 their median UPC values were as high or higher, and median SAlb values were as low or
562 lower, than those of dogs in other clusters. Also, dogs with MPGN had higher median
563 SCr values and hypertension more often than dogs in any other clusters. Third, although
564 dogs with glomerulosclerosis (Clusters 2 and 3) generally had the least severe
565 constellation of clinical abnormalities (lower median UPC values and SCr values and
566 higher median SAlb values than those of dogs in other clusters, with hypertension only
567 moderately often), the ranges of clinical data were large (Table 7). Finally, dogs with
568 amyloidosis (in Cluster 4) were hypertensive less often than dogs in any other cluster, but
569 they were otherwise more comparable to dogs with MGN (in Clusters 7 and 8) than to
570 dogs in any other clusters.

571 **DISCUSSION**

572 The purpose of this project was to objectively formulate a prototype scheme for
573 classification of glomerular diseases in proteinuric dogs.[13] While the human WHO
574 classification system for glomerular disease has been used to evaluate canine kidneys, the
575 validity of adopting the human classification scheme for canine patients has not been

assessed. Eight veterinary pathologists graded 114 parameters representing a wide array of glomerular, tubulointerstitial and vascular lesions examined with LM, TEM and IF. The dataset was analyzed by hierarchical cluster analysis, which enabled the development of an objectively derived prototype classification scheme. With this scheme now developed, a larger number of cases will be studied in the next phase to validate the classification system and to correlate pathologic findings with clinical and laboratory parameters and patient outcome.

The method of hierarchical cluster analysis, which included Wards linkage and L2 dissimilarity, works particularly well for the dataset created for this study because it performs best with clearly defined clusters and when there are few outliers.[39] The greatest dissimilarity between clusters is present at the top part of the dendrogram, where two distinct clusters emerged separating the patterns of predominantly non-immune-complex glomerular diseases (normal, amyloid, and FSGS) from patterns of immune-complex glomerular diseases (MPGN and MGN). Typically a bar parallel to the X-axis is drawn to denote the number of clusters at a particular level of dissimilarity. For our evaluation, a bar that delineates eight clusters was drawn, seven of which were distinguishable from the control cluster.

While these eight clusters encompass the most commonly observed patterns of glomerular lesions seen in dogs, there are a number of specific, but uncommon, diagnoses that were excluded from cluster analysis. In fact, after a preliminary dendrogram was created, seven cases with seemingly rare diagnoses were identified and excluded from analysis. Cluster analysis is an iterative process in which the investigator attempts to find a dendrogram pattern that makes physiologic (or pathophysiologic) sense. Exclusion of

599 these seven cases that appeared to be outliers resulted in a dendrogram that could be more
600 cogently interpreted.

601 Focal segmental glomerulosclerosis (FSGS) is a common morphologic pattern of
602 glomerular disease in humans with the nephrotic syndrome and is due to injury to the
603 glomerular visceral epithelial cell (podocyte). The podocyte plays a central role in
604 glomerular filtration permselectivity and responds to injury with reversible changes of
605 hypertrophy, foot process effacement, cell body attenuation, and microvillus formation.[21]
606 With continued injury, the podocyte irreversibly detaches from the outer aspect of the
607 GBM. Since the podocyte is a terminally differentiated cell with minimal proliferative
608 capability, podocyte loss results in hypertrophy of the remaining podocytes in order to
609 cover the denuded GBM. Experimental data indicates that if >40% of the podocytes are
610 lost the remaining podocytes are unable to cover the entire tuft.[51] Denuded areas of GBM
611 adhere to Bowman's capsule (synechiae), and the tuft undergoes segmental sclerosis or
612 scarring.

613 Podocyte loss and FSGS may be primary or secondary. Primary (or idiopathic)
614 FSGS is assumed to be due to innate defects in podocyte or slit diaphragm genes or
615 proteins. In humans, once a causative mutation is identified and the pathogenesis of
616 podocyte injury is elucidated, then that type of FSGS is considered to be secondary,
617 which is discussed below. While primary FSGS is a common morphologic pattern of
618 glomerular disease in people with the nephrotic syndrome, it has only recently been
619 recognized in dogs. Well-documented primary canine FSGS, with histopathologic,
620 immunofluorescence, and electron microscopic findings similar to the cases in this study,
621 was first described in 2010.[3] With the advent of improved renal diagnostics, the lesion of

622 primary FSGS has recently been recognized as a common cause of glomerular disease in
623 dogs. In a larger retrospective study, that also included cases used in this project, LM, IF,
624 and TEM evaluation of canine renal disease showed that FSGS was a common cause of
625 proteinuria accounting for 20.6% of the cases. In that group of dogs, FSGS was more
626 common than amyloidosis, which accounted for only 15.2% of the cases.[40] Recently,
627 genome-wide association studies of protein losing nephropathy of soft coated wheaten
628 terriers revealed mutations in two genes, NPHS1 and KIRREL2, encoding nephrin and
629 filtrin, respectively. These proteins are part of the podocyte slit diaphragm, and FSGS is
630 the dominant pathologic phenotype in proteinuric soft coated wheaten terriers; however
631 the exact pathogenesis of how this mutation interferes with podocyte function remains
632 unknown.[26] Similar genetic causes of primary / familial FSGS have been identified in
633 humans.

634 Secondary (or adaptive) FSGS is well-recognized in dogs with decreased
635 functional renal mass associated with naturally occurring chronic renal disease or
636 following experimental partial nephrectomy [7], and until relatively recently was thought to
637 be the only form of FSGS occurring in dogs. In this type of secondary FSGS, decreased
638 renal mass leads to glomerular hypertrophy and glomerular hyperfiltration of the
639 remaining nephrons. While these glomerular changes are initially adaptive responses that
640 increase glomerular filtration rate, they eventually become maladaptive causing podocyte
641 injury, podocyte detachment, and eventually glomerulosclerosis. Dogs with 11/12
642 nephrectomy and secondary glomerulosclerosis are azotemic (SCr 2.0 – 2.5 mg/dl) and
643 mildly proteinuric (mean UPC < 0.8) [8], in contrast to the variable occurrence of azotemia
644 and more profound proteinuria observed in dogs with primary FSGS. Similar

645 pathogeneses are likely occurring in cases of congenital nephron paucity, such as in dogs
646 with juvenile-onset nephropathies.

647 Secondary FSGS may also be caused by other types of injury to the podocyte.[36]
648 Immune-complex glomerulonephritis can induce podocyte injury and secondary
649 segmental glomerulosclerosis in humans and dogs, which leads to a diagnostic dilemma.
650 Cases with segmental sclerosis evaluated solely with LM might have histologically
651 undetectable immune-complex deposits in the capillary walls for which
652 immunosuppression would be recommended, emphasizing the importance of TEM and
653 IF. Hypertension is also known to injure podocytes and cause FSGS in humans and might
654 have a similar effect in some dogs. [14] Although obesity and hypertension have been
655 associated with proteinuria in dogs, [4,48] other studies have found conflicting results.[46] It is
656 important to realize that renal tissue was not consistently evaluated with advanced
657 diagnostic modalities in these veterinary studies so the association of hypertension and
658 obesity with FSGS requires further investigation.

659 All dogs in the FSGS group had similar lesions histologically, with increased
660 severity of lesions in Cluster 3 compared with Cluster 2. Cases in Cluster 3 had a
661 significantly greater percentage of glomeruli with sclerosis and significantly more
662 synechiae compared with Cluster 2. GBM hyalinosis, characterized by insudation of
663 plasma lipoproteins into the damaged capillary wall, and obsolescent glomeruli were also
664 more prevalent in Cluster 3. The co-existence of glomerular lipidosis encountered only
665 among cases of FSGS (clusters 2 and 3) was also noted. Glomerular lipidosis in dogs has
666 most often been reported as a sporadic, incidental glomerular change in kidneys which
667 otherwise lack significant pathology.[47,55] This association between glomerular lipidosis

668 and FSGS may change as larger numbers of cases are eventually considered, but its
669 occurrence in a small number of FSGS in this study suggests that glomerular lipidosis
670 may have pathologic significance. Future studies of the lesion of glomerular lipidosis in
671 dogs are warranted.

672 Seven cases within the FSGS group were exceptions to the ICGN vs non-ICGN
673 division of the dendrogram, because TEM revealed the presence of electron-dense
674 deposits. Review of these cases revealed that although electron-dense material consistent
675 with immune deposits was observed in the mesangium, involvement of the capillary
676 walls was absent or rare. The significance of having electron-dense deposits limited to the
677 mesangial regions is unknown; however, it is clear that the histopathologic pattern is one
678 of mesangial expansion, mesangial hypercellularity and segmental sclerosis as opposed to
679 endocapillary hypercellularity and remodeling of the glomerular basement membrane.
680 These seven cases might represent primary FSGS with secondary nonspecific trapping of
681 plasma constituents. Recent research in mice and humans has suggested that non-immune
682 mediated injury to the glomerulus can entrap circulating IgM, which can subsequently
683 activate the complement system leading to progressive glomerular injury.[43] Alternatively,
684 these seven cases could represent a sclerosing response of the glomerulus secondary to
685 previous mesangial deposition of immune complexes, similar to what occurs in the
686 sclerosing phenotype of mesangioproliferative IgA or C1q glomerulopathy in humans.
687 [30,53] Given that glomerulosclerosis, an irreversible lesion, was prominent in these seven
688 cases, whereas the electron-dense deposits were less so, it is justifiable to keep these
689 cases in the FSGS cluster. It is important to realize, however, that the presence of these
690 electron-dense deposits might exacerbate glomerular injury, and immunosuppressive

691 therapy might be a consideration in situations where standard therapies are unsuccessful.
692 The FSGS pattern raises three important points. First, FSGS is sufficient to result
693 in proteinuria, which can sometimes be severe. Second, because this disease begins as a
694 focal process, every glomerulus in a renal biopsy specimen should be examined. In
695 humans, approximately 20-25 glomeruli need to be evaluated to be able to confidently
696 rule out this diagnosis.[18] Third, and most importantly, the correct diagnosis of this lesion
697 is crucial because it can greatly influence treatment decisions.
698 Glomerular amyloidosis typically is not a diagnostic dilemma, although
699 occasional cases will have only minimal amyloid deposits. In these situations, the
700 diagnosis will rest upon the detection of small aggregates of fibrils with TEM and
701 negative IF results.
702 The ICGN branch of the dendrogram was comprised of four clusters, two of
703 which had MPGN patterns and two of which had MGN patterns. Membranoproliferative
704 glomerulonephritis is a pattern characterized by the presence of endocapillary
705 hypercellularity and double contours of the GBM. With rare exception (discussed below),
706 both lesions are due to the presence of subendothelial immune complexes. Theories have
707 been proposed for the pathogenesis of immune complex deposition, ranging from
708 entrapment of circulating immune complexes, to entrapment of a non-glomerular antigen
709 in the subendothelial space followed by eventual interaction with circulating antibody.[34]
710 Regardless of how they are deposited beneath the endothelium, it is their ability to
711 activate the complement cascade in proximity to the capillary lumen that results in a
712 hypercellular appearance. It is important to distinguish endocapillary hypercellularity
713 from mesangial hypercellularity when evaluating glomeruli. Endocapillary

714 hypercellularity consists of increased numbers of circulating inflammatory cells together
715 with hypertrophied or hyperplastic endothelial cells and / or interposed mesangial cells
716 within peripheral capillaries. In contrast, mesangial cell proliferation is confined to the
717 central mesangial matrix. Confusion arises because both endocapillary hypercellularity
718 and mesangial cell proliferation are not mutually exclusive lesions and because
719 evaluation of 5µm thick sections leads to overestimation of the number of nuclei within a
720 segment of the glomerular tuft. Use of the PAS stain and JMS method enabled the
721 pathologists to readily determine the location of the hypercellularity. While mesangial
722 proliferation was present in our cases of FSGS, endocapillary proliferation was not a
723 feature.

724 The PAS stain and JMS method also allowed the pathologists to discern between
725 GBM thickening and definitive double membrane contours, which are the result of
726 synthesis of new GBM material by the glomerular endothelium. The use of TEM and IF
727 verified the presence of immune complexes, thereby justifying a diagnosis of MPGN.
728 Importantly, there are diseases that demonstrate a MPGN pattern on histology without the
729 presence of immune complexes. Examples in humans include thrombotic
730 microangiopathy, [19] fibrillary glomerulonephritides, [1] and C3 glomerulopathy.[6,41] Of
731 these, thrombotic microangiopathy [9]and C3 glomerulopathy have been reported in
732 veterinary species.[2,5,37] Immunofluorescence and TEM are needed to differentiate
733 immune-complex MPGN from these rare diseases with alternate pathogeneses, because
734 therapeutic plans and prognoses depend on the correct diagnosis.

735 Membranous glomerulonephropathy is a pattern of injury caused by the presence
736 of immune complexes on the subepithelial (abluminal) side of the GBM. The presence of

737 a thickened GBM is insufficient to warrant this diagnosis. This represents a distinct shift
738 from the era in which MGN was diagnosed solely on the LM appearance of a thick
739 capillary wall. In the pattern of MGN proposed by the current study, the immune
740 complexes induce production of new GBM in between deposits (giving the appearance of
741 spikes), which eventually become encircled by new GBM. The encircled deposits take on
742 the appearance of clear holes when viewing by LM sections prepared by the JMS
743 method. Therefore GBM remodeling (spikes or holes) is a more important histologic
744 finding than thickened capillary walls. Because subepithelial immune complexes are
745 separated from the capillary lumen by GBM, endocapillary hypercellularity is minimal to
746 non-existent. One feature that separated Clusters 7 and 8 was the presence of segmental
747 sclerosis, which is presumed to be secondary to podocyte injury driven by the
748 subepithelial immune complexes. The subepithelial immune complexes activate
749 complement causing podocyte injury with podocyte foot process effacement and
750 increased loss of podocytes via C5b-9-mediated cellular injury.[35] Secondary segmental
751 glomerulosclerosis has prognostic significance in humans [35] and likely a similar
752 relationship might eventually be identified in dogs.
753 Cases from Cluster 5 and 8 were more severely affected, *i.e.,* had more severe
754 lesions) than Clusters 6 and 7, respectively. This might represent a greater impetus for
755 immune complex deposition or different stages of the diseases. Future studies will
756 investigate the relationship between underlying systemic diseases, which could be a
757 source of antigenemia. We did not detect significant associations between the
758 composition of immune-complex deposits as shown by the IF labeling and the various
759 patterns of histologic and ultrastructural lesions demonstrated by the LM and TEM

760 findings. Of interest, IgA staining was infrequent to rare (as opposed to the frequency of
761 IgA nephropathy in humans). We also did not identify cases of C3-only staining, which
762 would be supportive of a C3 glomerulopathy[6]. That does not mean that these types of
763 glomerular diseases do not exist in dogs, but merely that they were not identified in our
764 cohort of 89 cases. It remains necessary to perform a panel of IF staining so that
765 uncommon or rare diseases can be identified and properly investigated.
766 It is possible that the ICGN might represent a spectrum ranging from a pure
767 membranous form—with only subepithelial immune complexes and lacking
768 hypercellularity—to a pure membranoproliferative form with immune complexes located
769 solely in a subendothelial location and associated with fulminate inflammatory cell
770 accumulation. The middle portion of the spectrum may have both subepithelial and
771 subendothelial IC deposition with varying degrees of endocapillary hypercellularity. In
772 fact, this middle ground was previously diagnosed as Type III MPGN (Burkholder
773 variant) in both humans and dogs. The WHO classification of glomerular disease in
774 humans is currently in a state of reorganization, with the recent identification of
775 complementopathies and associated C3 glomerulopathies [41] as well as the development of
776 the International Society for Nephrology / Renal Pathology Society proposal for
777 classification of Lupus Nephritis.[29] This calls into question the validity of adopting
778 terminology such as Type III MPGN from a human nephropathology, when it is rarely
779 used and considered controversial. Therefore, we were very interested in how cases with
780 deposits in multiple locations would cluster in our cohort. Cluster analysis did not
781 separate out these "mixed cases" from purer patterns suggesting that the ultrastructural
782 localization of ICs was not a driving force for cluster grouping in this particular cohort of

783 patients. Determining whether or not canine cases will eventually be associated with an
784 underlying infection, complementopathy, or autoimmune disease is a future goal of this
785 initiative. It is possible that the variation in immune complex location will have etiologic
786 or prognostic implications. Therefore, we have opted to diagnose these cases as Mixed
787 MPGN and Mixed MGN so that the clinical presentation, progression and outcome of
788 these "variants" can be investigated.

789 Notably, cluster analysis based solely on the LM features of glomeruli resulted in a
790 strikingly different dendrogram with many misclassified cases. Seven of the eight MGN
791 cases in Cluster 8 incorrectly clustered with dogs without evidence of immune complex
792 deposition. Re-examination of these cases revealed fewer spikes and holes on the silver
793 stain and only mildly thickened GBMs. This demonstrates that GBM remodeling can be
794 subtle or absent in early cases of MGN and emphasizes the importance of additional
795 modalities for the correct diagnosis. Likewise, all of the cases from Cluster 3 were
796 incorrectly clustered with ICGN cases, likely because FSGS cases may have mesangial
797 hypercellularity and thickened capillary walls.

798 The main limitation of the study is that certain rare diseases had to be excluded
799 from the cluster analysis. Although this step was necessary to generate an interpretable
800 dendrogram, it also meant that we were unable to identify patterns associated with these
801 diagnoses. Additionally, the collection of renal biopsy material from control dogs was
802 difficult, as it is an invasive procedure. Therefore, we used tissue obtained during
803 ovariohysterectomy prior to adoption of racing greyhounds, which precluded any breed
804 or age matching with the case cohort. Lastly, certain clinical parameters such as
805 signalment, body condition score, and infectious disease exposure was not examined in

806 this study, as those data will be analyzed in future publications from the veterinary
807 nephrologists associated with the WSAVA-RSSG.
808 The question arises as to whether classification of these lesions by evaluation of a
809 large number of morphological parameters is worth the additional effort. Clearly, the
810 comparison of dendrogram in Figure 3 (only LM parameters) to that of Figure 2 (all
811 modalities) demonstrates the necessity of advanced diagnostics. Using only LM features
812 resulted in the misclassification that might have led to inappropriate treatment of 22 of 89
813 cases (25%). With the advent of immunosuppressive agents for ICGN, considerable care
814 should be taken to determine which patients will likely benefit from these therapeutic
815 regimens. It is also our opinion that valuable phenotypic data will be lost if the lesions
816 are not clearly defined and quantified. This lesion-based phenotypic approach could help
817 better categorize cases for epidemiologic analyses, investigation of molecular
818 pathogenesis, prognostication and treatment decisions. A similar approach is the basis of
819 the Nephrotic Syndrome Study Network (NEPTUNE) study, in which lesions identified
820 in renal biopsy specimens of nephrotic human patients are accurately phenotyped for
821 ongoing and future molecular tissue analysis.[15]
822 A number of the dogs in this study are part of an ongoing project designed to follow
823 clinical progression of disease after assessment of their renal biopsy using this
824 prototypical classification scheme. Biopsies of additional dogs enrolled in this
825 prospective study will be similarly evaluated, and outcome data will be analyzed.
826 The classification scheme that we propose in this study is intended to be modifiable
827 when outcome data becomes available from these ongoing incident cohort studies. In its
828 current form, however, our proposed clusters will facilitate communication among

clinicians and pathologists, whereas our list of lesions will clarify the terminology used in histopathologic descriptions. With this scheme in hand a larger number of cases (patients) will be studied in the next phase to validate the classification system and to correlate histological findings with clinical and clinical laboratory parameters and outcomes.

Footnotes:

[a] ScanScope CS, Aperio, Vista CA

[b] Spectrum, Aperio, Vista CA

[c] ImageScope CS, Aperio, Vista CA

[d] WebScope CS, Aperio, Vista CA

[e] GoToMeeting, Citrix Systems, Inc, Santa Barbara, CA

[f] Stata/IC 12 for Windows, StataCorp LP, College Station, TX

REFERENCES

1 Alpers CE, Kowalewska J: Fibrillary glomerulonephritis and immunotactoid glomerulopathy. *J Am Soc Nephrol* 2008:19(1):34-37.

2 Angus KW, Gardiner AC, Mitchell B, Thomson D: Mesangiocapillary glomerulonephritis in lambs: the ultrastructure and immunopathology of diffuse glomerulonephritis in newly born Finnish Landrace lambs. *J Pathol* 1980:131(1):65-74.

3 Aresu L, Zanatta R, Luciani L, Trez D, Castagnaro M: Severe renal failure in a dog resembling human focal segmental glomerulosclerosis. *J Comp Pathol* 2010:143(2-3):190-194.

4 Bacic A, Kogika MM, Barbaro KC, Iuamoto CS, Simoes DM, Santoro ML: Evaluation of albuminuria and its relationship with blood pressure in dogs with chronic kidney disease. *Vet Clin Pathol* 2010:39(2):203-209.

5 Blum JR, Cork LC, Morris JM, Olson JL, Winkelstein JA: The clinical manifestations of a genetically determined deficiency of the third component of complement in the dog. *Clin Immunol Immunopathol* 1985:34(3):304-315.

6 Bomback AS, Appel GB: Pathogenesis of the C3 glomerulopathies and reclassification of MPGN. *Nat Rev Nephrol* 2012:8(11):634-642.

7 Brown SA, Crowell WA, Brown CA, Barsanti JA, Finco DR: Pathophysiology and management of progressive renal disease. *Vet J* 1997:154(2):93-109.

8 Brown SA, Finco DR, Brown CA, Crowell WA, Alva R, Ericsson GE, et al.: Evaluation of the effects of inhibition of angiotensin converting enzyme with enalapril in dogs with induced chronic renal insufficiency. *Am J Vet Res* 2003:64(3):321-

327.
9 Carpenter JL, Andelman NC, Moore FM, King NW, Jr.: Idiopathic cutaneous and renal glomerular vasculopathy of greyhounds. *Vet Pathol* 1988:25(6):401-407.
10 Center SA, Smith CA, Wilkinson E, Erb HN, Lewis RM: Clinicopathologic, renal immunofluorescent, and light microscopic features of glomerulonephritis in the dog: 41 cases (1975-1985). *J Am Vet Med Assoc* 1987:190(1):81-90.
11 Cianciolo RE, Brown CA, Mohr FC, Spangler WL, Aresu L, van der Lugt JJ, et al.: Pathologic Evaluation of Canine Renal Biopsies: Methods for Identifying Features that Differentiate Immune-Mediated Glomerulonephritides from Other Categories of Glomerular Diseases. *Journal of Veterinary Internal Medicine* 2013:27:S10-S18.
12 Cook AK, Cowgill LD: Clinical and pathological features of protein-losing glomerular disease in the dog: a review of 137 cases (1985-1992). *J Am Anim Hosp Assoc* 1996:32(4):313-322.
13 Cowgill LD, Polzin DJ: Vision of the WSAVA Renal Standardization Project. *Journal of Veterinary Internal Medicine* 2013:27:S5-S9.
14 D'Agati VD: The spectrum of focal segmental glomerulosclerosis: new insights. *Curr Opin Nephrol Hypertens* 2008:17(3):271-281.
15 Gadegbeku CA, Gipson DS, Holzman LB, Ojo AO, Song PX, Barisoni L, et al.: Design of the Nephrotic Syndrome Study Network (NEPTUNE) to evaluate primary glomerular nephropathy by a multidisciplinary approach. *Kidney Int* 2013:83(4):749-756.
16 Harris CH, Krawiec DR, Gelberg HB, Shapiro SZ: Canine IgA glomerulonephropathy. *Veterinary Immunology and Immunopathology* 1993:36(1):1-16.
17 Jaenke RS, Allen TA: Membranous nephropathy in the dog. *Vet Pathol* 1986:23(6):718-733.
18 Jennette JCS, M. M.; Olson, J. L.; Silva, F. G.: Primer on the Pathologic Diagnosis of Renal Disease. In: Jennette JCO, J. L.; Schwartz, M. M.; Silva F. G., ed. *Heptistall's Pathology of the Kidney*. 6th ed. Philadelphia, PA: Lippincott Williams & Wilkins; 2007: 97-123.
19 Keir L, Coward RJ: Advances in our understanding of the pathogenesis of glomerular thrombotic microangiopathy. *Pediatr Nephrol* 2011:26(4):523-533.
20 Koeman JP, Biewenga WJ, Gruys E: Proteinuria in the dog: a pathomorphological study of 51 proteinuric dogs. *Res Vet Sci* 1987:43(3):367-378.
21 Kriz W, Shirato I, Nagata M, LeHir M, Lemley KV: The podocyte's response to stress: the enigma of foot process effacement. *Am J Physiol Renal Physiol* 2013:304(4):F333-347.
22 Kurtz JM, Russell SW, Lee JC, Slauson DO, Schechter RD: Naturally occurring canine glomerulonephritis. *Am J Pathol* 1972:67(3):471-482.
23 Lees GE, Brown SA, Elliott J, Grauer GE, Vaden SL: Assessment and management of proteinuria in dogs and cats: 2004 ACVIM Forum Consensus Statement (small animal). *J Vet Intern Med* 2005:19(3):377-385.
24 Lewis RJ: Canine glomerulonephritis: results from a microscopic evaluation of

fifty cases. *Can Vet J* 1976:17(7):171-176.
25 Littman MP, Daminet S, Grauer GF, Lees GE, van Dongen AM: Consensus recommendations for the diagnostic investigation of dogs with suspected glomerular disease. *J Vet Intern Med* 2013:27 Suppl 1:S19-26.
26 Littman MP, Wiley CA, Raducha MG, Henthorn PS: Glomerulopathy and mutations in NPHS1 and KIRREL2 in soft-coated Wheaten Terrier dogs. *Mamm Genome* 2013:24(3-4):119-126.
27 Macdougall DF, Cook T, Steward AP, Cattell V: Canine chronic renal disease: prevalence and types of glomerulonephritis in the dog. *Kidney Int* 1986:29(6):1144-1151.
28 Marino CL, Cober RE, Iazbik MC, Couto CG: White-coat effect on systemic blood pressure in retired racing Greyhounds. *J Vet Intern Med* 2011:25(4):861-865.
29 Markowitz GS, D'Agati VD: The ISN/RPS 2003 classification of lupus nephritis: an assessment at 3 years. *Kidney Int* 2007:71(6):491-495.
30 Mii A, Shimizu A, Masuda Y, Fujita E, Aki K, Ishizaki M, et al.: Current status and issues of C1q nephropathy. *Clin Exp Nephrol* 2009:13(4):263-274.
31 Miyauchi Y, Nakayama H, Uchida K, Uetsuka K, Hasegawa A, Goto N: Glomerulopathy with IgA deposition in the dog. *J Vet Med Sci* 1992:54(5):969-975.
32 Muller-Peddinghaus R, Trautwein G: Spontaneous glomerulonephritis in dogs. I. Classification and immunopathology. *Vet Pathol* 1977:14(1):1-13.
33 Murray M, Wright NC: A morphologic study of canine glomerulonephritis. *Lab Invest* 1974:30(2):213-221.
34 Nangaku M, Couser WG: Mechanisms of immune-deposit formation and the mediation of immune renal injury. *Clin Exp Nephrol* 2005:9(3):183-191.
35 Nangaku M, Shankland SJ, Couser WG: Cellular response to injury in membranous nephropathy. *J Am Soc Nephrol* 2005:16(5):1195-1204.
36 Noël LH: Morphological features of primary focal and segmental glomerulosclerosis. *Nephrology Dialysis Transplantation* 1999:14(suppl 3):53-57.
37 Reusch C, Hoerauf A, Lechner J, Kirsch M, Leuterer G, Minkus G, et al.: A new familial glomerulonephropathy in Bernese mountain dogs. *Vet Rec* 1994:134(16):411-415.
38 Rouse BT, Lewis RJ: Canine glomerulonephritis: prevalence in dogs submitted at random for euthanasia. *Can J Comp Med* 1975:39(4):365-370.
39 Sarstedt M, Mooi E: *A Concise Guide to Market research: The process, data, and methods using IBM SPSS statistics*: Springer Verlag, 2011.
40 Schneider SM, Cianciolo RE, Nabity MB, Clubb FJ, Jr., Brown CA, Lees GE: Prevalence of immune-complex glomerulonephritides in dogs biopsied for suspected glomerular disease: 501 cases (2007-2012). *J Vet Intern Med* 2013:27 Suppl 1:S67-75.
41 Sethi S, Fervenza FC: Membranoproliferative glomerulonephritis: pathogenetic heterogeneity and proposal for a new classification. *Semin Nephrol* 2011:31(4):341-348.
42 Slauson DO, Lewis RM: Comparative pathology of glomerulonephritis in animals. *Vet Pathol* 1979:16(2):135-164.

43 Strassheim D, Renner B, Panzer S, Fuquay R, Kulik L, Ljubanovic D, et al.: IgM contributes to glomerular injury in FSGS. *J Am Soc Nephrol* 2013:24(3)**:**393-406.
44 Stuart BP, Phemister RD, Thomassen RW: Glomerular lesions associated with proteinuria in clinically healthy dogs. *Vet Pathol* 1975:12(2)**:**125-144.
45 Surman S, Couto CG, Dibartola SP, Chew DJ: Arterial blood pressure, proteinuria, and renal histopathology in clinically healthy retired racing greyhounds. *J Vet Intern Med* 2012:26(6)**:**1320-1329.
46 Tefft KM, Shaw DH, Ihle SL, Burton SA, Pack L: Association between excess body weight and urine protein concentration in healthy dogs. *Vet Clin Pathol* 2014:43(2)**:**255-260.
47 Thiel W, Hartig F, Frese K: Glomerular lipidosis in the dog. *Exp Pathol* 1981:19(3)**:**154-160.
48 Tvarijonaviciute A, Ceron JJ, Holden SL, Cuthbertson DJ, Biourge V, Morris PJ, et al.: Obesity-related metabolic dysfunction in dogs: a comparison with human metabolic syndrome. *BMC Vet Res* 2012:8**:**147.
49 Vilafranca M, Wohlsein P, Leopold-Temmler B, Trautwein G: A canine nephropathy resembling minimal change nephrotic syndrome in man. *J Comp Pathol* 1993:109(3)**:**271-280.
50 Vilafranca M, Wohlsein P, Trautwein G, Leopold-Temmler B, Nolte I: Histological and Immunohistological Classification of Canine Glomerular Disease. *Journal of Veterinary Medicine Series A* 1994:41(1-10)**:**599-610.
51 Wharram BL, Goyal M, Wiggins JE, Sanden SK, Hussain S, Filipiak WE, et al.: Podocyte depletion causes glomerulosclerosis: diphtheria toxin-induced podocyte depletion in rats expressing human diphtheria toxin receptor transgene. *J Am Soc Nephrol* 2005:16(10)**:**2941-2952.
52 Wright NG, Nash AS, Thompson H, Fisher EW: Membranous nephropathy in the cat and dog: a renal biopsy and follow-up study of sixteen cases. *Lab Invest* 1981:45(3)**:**269-277.
53 Wyatt RJ, Julian BA: IgA nephropathy. *N Engl J Med* 2013:368(25)**:**2402-2414.
54 Yhee JY, Yu CH, Kim JH, Im KS, Chon SK, Sur JH: Histopathological retrospective study of canine renal disease in Korea, 2003∼2008. *J Vet Sci* 2010:11(4)**:**277-283.
55 Zayed I, Gopinath C, Hornstra HW, Spit BJ, Heijden CA: A light and electron microscopical study of glomerular lipoidosis in beagle dogs. *J Comp Pathol* 1976:86(4)**:**509-517.

Table 1a. Parameter Identification and Method of Scoring: Light Microscopy

Light Microscopy	Scoring method	Light Microscopy	Scoring method	Light Microscopy	Scoring method
Endocapillary hypercellularity	Severity 0-1-2-3-4	Arteriolar MHH	Frequency (%)	Dilation of Bowman's capsule	Frequency (%)
Hypercellularity from neutrophils	Severity 0-1-2-3-4	Arteriolar hyalinosis	Frequency (%)	Fibrin in Bowman's space	Frequency (%)
Mesangial hypercellularity	Severity 0-1-2-3-4	Glom. inflammatory cells	Frequency (%)	Periglomerular inflammation	Frequency (%)
Amyloid	Severity 0-1-2-3-4	Podocyte hypertrophy	Frequency (%)	Periglomerular fibrosis	Frequency (%)
Capillary loop thickening	Severity 0-1-2-3-4	Podocyte hyperplasia	Frequency (%)	Tubular lumen dilation	Frequency (%)
Immune deposits	Severity 0-1-2-3-4	Podocyte vacuoles	Frequency (%)	Tubular atrophy	Frequency (%)
GBM spikes	Severity 0-1-2-3-4	Podocyte protein droplets	Frequency (%)	Tubular epith. single cell necrosis	Frequency (%)
GBM holes	Severity 0-1-2-3-4	GBM duplication	Frequency (%)	Tubular necrosis	Frequency (%)
Synechiae	Severity 0-1-2-3-4	Synechiae	Frequency (%)	Tubular regeneration	Frequency (%)
GBM hyalinosis	Severity 0-1-2-3-4	Obsolescent glomeruli	Frequency (%)	Hyaline (protein) casts	Frequency (%)
Interstitial edema	Severity 0-1-2-3-4	Glomerular lipidosis	Frequency (%)	Tubular proteinosis	Frequency (%)
Interstitial amyloid	Severity 0-1-2-3-4	Glomerular thrombi	Frequency (%)	Intratubular cellular casts	Frequency (%)
Interstitial hemorrhage	Severity 0-1-2-3-4	Capill. aneurysmal dilation	Frequency (%)	Intratubular crystals	Frequency (%)
Amyloid in vascular walls	Severity 0-1-2-3-4	Glom. tuft nuclear debris	Frequency (%)	Intratubular pigment	Frequency (%)
Interstitial small artery MHH	Absence (0), Presence (1)	GBM wrinkling	Frequency (%)	Tubulitis	Frequency (%)
Interstitial small artery hyalinosis	Absence (0), Presence (1)	GBM hyalinosis	Frequency (%)	Tubular rupture	Frequency (%)
Interstitial large artery MHH	Absence (0), Presence (1)	Kimmelstiel-Wilson nodules	Frequency (%)	Tubular epith. cell vesiculation	Frequency (%)
Interstitial large artery hyalinosis	Absence (0), Presence (1)	Parietal cell hypertrophy	Frequency (%)	Tubular epith. cell isometric vesicul.	Frequency (%)
Degree of mesangial matrix expansion	Extent 0-1-2-3-4	Parietal cell hyperplasia	Frequency (%)	Tubular epith. cell protein droplets	Frequency (%)
Percent mesangial matrix expansion	Frequency (%)	Parietal cell protein droplets	Frequency (%)	Tubular epithelial cell pigment	Frequency (%)
Degree of glomerulosclerosis	Extent 0-1-2-3-4	Crescents	Frequency (%)	Percent interstitial fibrosis	Frequency (%)
Percent glomerulosclerosis	Frequency (%)	Symm. Bowman's cap. thick.	Frequency (%)	Percent interstitial inflammation	Frequency (%)
Hilar glomerulosclerosis	Frequency (%)	Asymm. Bowman's cap. thick.	Frequency (%)	Interstitial fibrosis	Severity 0-1-2-3
Tip glomerulosclerosis	Frequency (%)	Bowman's capsule BM splitting	Frequency (%)	Interstitial inflammation	Severity 0-1-2-3
Glomerulosclerosis not at poles	Frequency (%)	Bowman's capsule BM mineral.	Frequency (%)		
Glomerulosclerosis location undet	Frequency (%)	Fetal glomeruli	Frequency (%)		

Parameters selected for the 59-parameter dataset are underlined. See the text for a description of the grading schemes. Note some parameters appear twice in table because data was collected for both frequency and severity or extent. GBM: glomerular basement membrane, MHH: medial hypertrophy/hyperplasia, Undet: undetermined, BM: basement membrane.

Table 1b. Parameter Identification and Method of Scoring for Transmission Electron Microscopy and Immunofluorescence Microscopy

Transmission Electron Microscopy	Scoring method	Transmission Electron Microscopy	Scoring method	Immunofluorescence microscopy	Scoring method
Subepithelial electron-dense deposits	Prevalence 0-1-2	Mesangial cell interpositioning	Occurrence 0-1	IgG mesangium	GranLbl 0-1-2
Subendothelial electron-dense deposits	Prevalence 0-1-2	Amyloid fibrils	Occurrence 0-1	IgG capillary wall	GranLbl 0-1-2
Mesangial electron-dense deposits	Prevalence 0-1-2	Other fibrils	Occurrence 0-1	IgM mesangium	GranLbl 0-1-2
Paramesangial electron-dense deposits	Prevalence 0-1-2	Podocyte microvillus transformation	Occurrence 0-1	IgM capillary wall	GranLbl 0-1-2
Intramem. electron-dense deposits	Prevalence 0-1-2	Podocyte cytoplasmic vacuoles	Occurrence 0-1	IgA mesangium	GranLbl 0-1-2
GBM spikes	Prevalence 0-1-2	Podocyte myelin figures	Occurrence 0-1	IgA capillary wall	GranLbl 0-1-2
Encircled electron-dense deposits	Prevalence 0-1-2	Podocyte swelling	Occurrence 0-1	C3 mesangium	GranLbl 0-1-2
Encircled deposits with dissolution	Prevalence 0-1-2	Endothelial cell swelling	Occurrence 0-1	C3 capillary wall	GranLbl 0-1-2
Podocyte foot process effacement	Prevalence 0-1-2	Tubuloreticular inclusions	Occurrence 0-1		
GBM thinning	Prevalence 0-1-2	Endothelial cell cytoplasmic vacuoles	Occurrence 0-1		
GBM splitting	Prevalence 0-1-2	Endothelial cell myelin figures	Occurrence 0-1		
GBM rarefaction	Prevalence 0-1-2	Intravascular inflammatory cells	Occurrence 0-1		
Subendothelial widening	Prevalence 0-1-2	Mesangial cell cytoplasmic vacuoles	Occurrence 0-1		
Diffuse GBM thickening	Prevalence 0-1-2	Mesangial cell myelin figures	Occurrence 0-1		
GBM wrinkling	Prevalence 0-1-2	Mesangial electron dense material	Occurrence 0-1		

Parameters selected for the 59-parameter set are underlined. GranLbl indicates positive fluorescent labeling in a granular pattern consistent with the presence of immune deposits.

Table 2. Parameter Scores for Whole Renal Biopsy Evaluation by Light Microscopy

PATTERN OF INJURY	Cluster 1 (Control)	Cluster2 (FSGS)	Cluster 3 (FSGS)	Cluster 4 (Amyloidosis)	Cluster 5 (MPGN)	Cluster 6 (MPGN)	Cluster 7 (MGN)	Cluster 8 (MGN)
Endocapillary hypercellularity	0.0 (00-0.0)	0.3 (0.0-0.8)	0.5 (0.0-2.0)	0.0 (0.0-0.3)	3.0 (0.7-3.9)	2.4 (1.8-4.0)	0.7[a] (0.0-2.8)	0.1 (0.0-1.0)
Mesangial hypercellularity	0.4 (0.4-0.7)	1.6 (0.8-2.0)	2.1[b] (1.3-2.9)	0.6 (0.0 -1.0)	2.8 (2.4-3.4)	2.6 (1.1-3.3)	2.0[b] (1.1-3.0)	1.3 (0.3-1.9)
Hypercellularity from neutrophils	0.0 (0.0-0.0)	0.0 (0.0-0.6)	0.3[a] (0.0-0.8)	0.0 (0.0-0.6)	1.5 (0.1-2.8)	1.1 (0.0-2.8)	0.3[a] (0.0-1.3)	0.0 (0.0-0.4)
Synechiae	0.1 (0.0-0.7)	1.8 (0.8-2.0)	3.0[d] (2.0-3.4)	1.2 (0.4-4.0)	3.0[d] (2.3-4.0)	1.6 (0.6-2.8)	2.5[c] (1.3-3.0)	1.1 (0.5-2.0)
Hyalinosis	0.0 (0.0-0.6)	1.0 (0.0-1.7)	2.0[c] (0.3-3.4)	0.0 (0.0-0.3)	3.2[d] (2.0-3.8)	0.8 (0.0-1.6)	1.0[a] (0.3-2.0)	0.3 (0.0-1.3)
Capill. Loop thickening	0.0 (0.0-0.1)	1.0 (0.3-1.8)	1.8[c] (0.8-2.6)	0.8 (0.3-3.0)	2.9 (1.4-4.0)	2.5 (1.5-3.0)	3. 0[d] (2.3-3.8)	1.7 (1.1-2.3)
Immune Deposits[1]	0.0 (0.0-0.0)	0.0 (0.0-0.4)	0. 0 (0.0-0.1)	0.0 (0.0-0.0)	0.4 (0.0-1.9)	0.3 (0.0-2.4)	2.3[a] (0.7-3.7)	1.6 (0.0-3.0)
GBM spikes	0.0 (0.0-0.0)	0.0 (0.0-0.0)	0.0 (0.0-1.0)	0. 0 (0.0 -0.0)	0.0 (0.0-0.8)	0.3 (0.0-0.8)	2.4[c] (2.0-3.8)	0.9 (0.1-2.4)
GBM holes	0.0 (0.0-0.0)	0.0 (0.0-0.3)	0.0[a] (0.0-0.5)	0.0 (0.0-0.0)	0.0 (0.0-0.5)	0.3 (0.0-0.8)	1.8[c] (0.3-2.8)	0.2 (0.0-1.0)
Amyloid	0.0 (0.0-0.0)	0.0 (0.0-0.0)	0.0 (0.0-0.0)	3.0 (1.9-4.0)	0.0 (0.0 -0.0)	0.0 (0.0-0.0)	0.0 (0.0-0.0)	0.0 (0.0-0.0)
Mesang. Matrix expan.	0.2 (0.0-0.5)	0.9 (0.4-3.0)	1.8[b] (1.0-2.3)	2.8 (1.8-3.8)	2.7 (2.0-3.0)	2.0 (0.8-3.0)	1.1 (0.5-2.7)	0.8 (0.0-1.8)
Degree of sclerosis[2]	0.0 (0.0-0.0)	0.3 (0.0-1.4)	1.3[c] (0.9-2.6)	0.0 (0.0-0.0)	1.2 (0.0-3.3)	0.5 (0.1-1.8)	0.6[b] (0.0-2.1)	0.1 (0.0-0.9)

Interstitial Small Arterial MHH[3]	0.0 (0.0-0.0)	0.3 (0.0-0.8)	0.8[b] (0.1-1.0)	0.0 (0.0-0.5)	0.5 (0.0-1.0)	0.6 (0.0-1.0)	0.5[a] (0.0-1.0)	0.0 (0.0-0.6)
Interstitial fibrosis[4]	0.0 (0.0-0.0)	0.5 (0.0-1.6)	0.5 (0.2-1.7)	0.3 (0.0-1.4)	0.8 (0.1-1.7)	0.3 (0.1-0.9)	0.4[a] (0.0-1.2)	0.1 (0.0-0.4)
Interstitial inflammation[4]	0.0 (0.0-0.3)	0.4 (0.0-1.2)	0.8[a] (0.2-1.8)	0.2 (0.0-0.9)	1.0[b] (0.6-1.4)	0.5 (0.3-1.3)	0.6 (0.0-1.4)	0.3 (0.0-1.0)

Values were medians with (Minimum and Maximum values) and were based on scores that range from 0-4 with exceptions noted below. All parameter listed were part of the 59-parameter dataset. GBM: glomerular basement membrane, MHH: medial hypertrophy/hyperplasia. [1]Fuchsinophilic deposits with Masson trichrome staining. [2]Criteria based on distribution of sclerosis in the glomerular tuft (0, no sclerosis, 1, <25%; 2, 25-50; 3, 51-75%; 4, > 75% involvement). [3]Values were based on a 0 (absent) or 1 (present) scale. [4]Values represented the character of either interstitial fibrosis or inflammation (no fibrosis/inflammation, no distortion of architecture by fibrosis/inflammation, separation of tubules by fibrosis/inflammation, and replacement of tubules by fibrosis/inflammation) and were graded on 0-3 scale. [a]$p < 0.05$, [b]$p<0.01$, [c]$p<0.001$, [d]$p<0.0001$ with comparisons made between Clusters 2 and 3 or Clusters 5 and 6 or Clusters 7 and 8.

Table 3. Parameter Scores for Individual Glomeruli and Tubulointerstitial Fields by Light Microscopy

PATTERN OF INJURY	Cluster 1 (Control)	Cluster 2 (FSGS)	Cluster 3 (FSGS)	Cluster 4 (Amyloidosis)	Cluster 5 (MPGN)	Cluster 6 (MPGN)	Cluster 7 (MGN)	Cluster 8 (MGN)
GBM hyalinosis	2 (0-7)	11 (0-28)	21 (0-66)	5 (0-14)	63[c] (27-95)	17 (0-41)	19[b] (0-63)	3 (0-19)
Synechiae	6 (0-14)	28 (14-65)	60[b] (39-86)	42 (13-100)	73[b] (50-86)	51 (12-76)	43[b] (9-75)	26 (16-50)
Percent mesangial matrix expansion	25 (0-45)	63 (28-100)	82[a] (55-94)	97 (79-100)	95 (85-100)	85 (50-100)	74 (31-100)	50 (0-93)
Percent glomerulosclerosis	0 (0-0)	28 (3-60)	72[c] (47-100)	0 (0-0)	61 (0-100)	35 (3-75)	33[b] (0-95)	9 (0-58)
Obsolescent glomeruli	0 (0-0)	7 (0-33)	22[b] (0-43)	4 (0-25)	7 (0-38)	2 (0-13)	8 (0-28)	2 (0-12)
Nuclear debris	1 (0-4)	8 (0-25)	20[b] (0-42)	24 (5-75)	43 (19-73)	36 (0-73)	21 (0-69)	10 (0-36)
Periglomerular inflammation	3 (0-11)	8 (0-30)	30[b] (3-75)	15 (0-39)	43 (15-82)	27 (0-72)	22 (0-55)	17 (0-74)
Periglomerular fibrosis	3 (0-7)	12 (0-33)	19 (0-50)	11 (0-50)	51[b] (15-86)	18 (0-50)	14 (0-56)	4 (0-15)
Parietal cell hypertrophy	6 (0-14)	27 (9-58)	36 (19-60)	24 (9-63)	60 (21-85)	46 (13-75)	34 (10-58)	33 (14-56)
Parietal cell hyperplasia	4 (0-14)	14 (0-44)	24 (6-58)	18 (0-75)	44[b] (25-62)	27 (12-50)	21 (10-34)	18 (0-50)
Glomerular inflammatory cells	3 (0-7)	7 (0-27)	9 (0-25)	10 (0-33)	42 (8-73)	39 (0-91)	12 (0-50)	12 (0-29)
GBM duplication	3 (0-11)	7 (0-37)	12 (0-43)	6 (0-38)	40 (13-58)	45 (9-82)	20 (0-67)	20 (0-75)
Bowman's capsule Basement membrane splitting	10 (0-18)	15 (0-43)	20 (6-38)	7 (0-25)	40[c] (0-75)	13 (0-28)	17[a] (0-63)	4 (0-15)
Tubular epithelial single cell necrosis	1 (0-4)	22 (0-67)	34 (9-58)	32 (8-67)	44 (17-71)	33 (5-67)	23 (0-50)	18 (0-61)
Tubular regeneration	2 (0-7)	11 (0-35)	12 (0-30)	15 (0-33)	26 (0-57)	18 (0-44)	11 (0-39)	11 (0-21)

Tubular epithelial cell pigment	19 (4-50)	27 (0-73)	38 (7-79)	30 (8-96)	26 (0-63)	50 (4-100)	37 (4-75)	35 (0-81)
Tubular epithelial cell isometric vesiculation	9 (0-21)	7 (0-33)	7 (0-20)	11 (0-93)	8 (0-33)	6 (0-32)	4 (0-14)	18[a] (0-42)
Arteriolar hyalinosis[1]	0 (0-0)	11 (0-67)	16 (0-47)	1 (0-7)	34[b] (0-75)	7 (0-33)	6 (0-43)	5 (0-20)
Interstitial fibrosis[2]	0 (0-0)	9 (0-34)	8 (1-25)	6 (0-31)	11[b] (1-35)	2 (0-4)	5[a] (0-28)	1 (0-3)
Interstitial inflammation[2]	0 (0-1)	3 (0-9)	9[a] (1-20)	3 (0-12)	7[c] (3-11)	3 (1-6)	3 (0-7)	2 (0-10)

Values were means percent with (Minimum and Maximum values) and were based on scoring a range of 4-32 glomeruli. All parameters listed were part of the 59-parameter dataset. [1]Both afferent and efferent arterioles. [2]Interstitial fibrosis and inflammation based on percentage of fields affected. [a]$p < 0.05$, [b]$p<0.01$, [c]$p<0.001$ with comparisons made between Clusters 2 and 3 or Clusters 5 and 6 or Clusters 7 and 8.

Table 4. Parameter Scores for Electron-Dense Deposit Location and Glomerular Basement Membrane Remodeling Evaluated by TEM

PATTERN OF INJURY	Cluster1 (Control)	Cluster 2 (FSGS)	Cluster 3 (FSGS)	Cluster 4 (Amyloidosis)	Cluster 5 (MPGN)	Cluster 6 (MPGN)	Cluster 7 (MGN)	Cluster 8 (MGN)
Subepithelial electron-dense deposits	0.0 (0.0-0.0)	0.0 (0.0-0.0)	0.0 (0.0-0.0)	0.0 (0.0-0.0)	0.0 (0.0-2.0)	2.0[a] (0.0-2.0)	2.0 (1.0-2.0)	2.0 (2.0-2.0)
Subendothelial electron-dense deposits	0.0 (0.0-0.0)	0.0 (0.0-2.0)	0.0 (0.0-0.0)	0.0 (0.0-0.0)	2.0 (2.0-2.0)	2.0 (2.0-2.0)	0.0 (0.0-2.0)	0.0 (0.0-2.0)
Mesangial electron-dense deposits	0.0 (0.0-0.0)	0.0 (0.0-2.0)	0.0 (0.0-2.0)	0.0 (0.0-0.0)	2.0 (0.0-2.0)	2.0[a] (2.0-2.0)	2.0 (0.0-2.0)	0.5 (0.0-2.0)
Paramesangial electron-dense deposits	0.0 (0.0-0.0)	0.0 (0.0-0.0)	0.0 (0.0-0.0)	0.0 (0.0-0.0)	0.0 (0.0-2.0)	2.0[a] (0.0-2.0)	2.0 (1.0-2.0)	2.0 (1.0-2.0)
Intramembranous electron-dense deposits	0.0 (0.0-0.0)	0.0 (0.0-0.0)	0.0 (0.0-1.0)	0.0 (0.0-0.0)	1.0 (0.0-2.0)	1.0 (0.0-2.0)	2.0[a] (1.0-2.0)	1.0 (0.0-2.0)
GBM spikes	0.0 (0.0-0.0)	0.0 (0.0-0.0)	0.0 (0.0-0.0)	0.0 (0.0-0.0)	0.0 (0.0-0.0)	1.0[b] (0.0-2.0)	2.0[a] (1.0-2.0)	1.0 (0.0-2.0)
Encircled electron-dense deposits	0.0 (0.0-0.0)	0.0 (0.0-0.0)	0.0 (0.0-0.0)	0.0 (0.0-0.0)	0.0 (0.0-1.0)	0.0 (0.0-2.0)	2.0[a] (1.0-2.0)	1.0 (0.0-2.0)

Values were medians with (Minimum and Maximum values) and were based on scores ranging from 0-2 (0, absent; 1, rare; 2, not rare). All parameters listed were part of the 59-parameter dataset. [a]$p < 0.05$, [b]$p<0.01$ with comparisons made between Clusters 2 and 3 or Clusters 5 and 6 or Clusters 7 and 8.

Table 5. Parameter Scores for Glomeruli Evaluated by TEM

PATTERN OF INJURY	Cluster 1 (Control)	Cluster 2 (FSGS)	Cluster 3 (FSGS)	Cluster 4 (Amyloidosis)	Cluster 5 (MPGN)	Cluster 6 (MPGN)	Cluster 7 (MGN)	Cluster 8 (MGN)
Mesangial cell interpositioning	0.43 (O.00-0.43)	0.75 (0.00-1.00)	0.86 (0.25-1.00)	0.00 (0.00-0.50)	1.00 (0.88-1.00)	1.00 (0.75-1.00)	0.75 (0.25-1.00)	0.63 (0.00-1.00)
Endothelial cell swelling	0.00 (0.00-0.00)	0.00 (0.00-0.50)	0.00 (0.00-0.25)	0.00 (0.00-0.14)	0.50 (0.29-1.00)	0.29 (0.13-0.75)	0.00 (0.00-0.50)	0.00 (0.00-0.83)
Diffuse GBM thickening	0.00 (0.00-0.00)	0.00 (0.00-0.75)	0.25[a] (0.00-1.00)	0.00 (0.00-01.00)	0.00 (0.00-0.43)	0.13 (0.00-0.57)	0.25[a] (0.00-0.75)	0.00 (0.00-0.43)
Intravascular inflammatory cells	0.00 (0.00-014)	0.00 (0.00-0.50)	0.00 (0.00-0.50)	0.00 (0.00-0.38)	0.25 (0.00-0.71)	0.25 (0.00-0.75)	0.00 (0.00-0.25)	0.06 (0.00-0.14)
GBM rarefaction	0.29 (0.14-0.43)	0.38 (0.00-0.75)	0.50 (0.00-0.75)	0.07 (0.00-0.50)	0.20 (0.00-0.67)	0.13 (0.00-0.50)	0.25 (0.00-0.57)	0.13 (0.00-0.57)
GBM wrinkling	0.43 (0.00-0.71)	0.43 (0.00-0.88)	0.50 (0.00-1.00)	0.15 (0.00-0.75)	0.43 (0.13-1.00)	0.25 (0.00-0.50)	0.25 (0.00-0.60)	0.13 (0.00-0.38)
Podocyte microvillous transformation	0.00 (0.00-0.00)	0.25 (0.00-1.00)	0.50 (0.00-0.86)	0.25 (0.00-1.00)	0.50 (0.00-071)	0.50 (0.00-0.88)	0.75 (0.00-1.00)	0.80 (0.38-1.00)
Endothelial cell cytoplasmic vacuoles	0.00 (0.00-0.00)	0.00 (0.00-0.75)	0.25 (0.00-0.75)	0.00 (0.00-0.25)	0.21 (0.00-0.80)	0.25 (0.00-0.43)	0.00 (0.00-0.25)	0.13 (0.00-0.33)
Amyloid fibrils	0.00 (0.00-0.00)	0.00 (0.00-0.00)	0.00 (0.00-0.13)	1.00 (1.00-1.00)	0.00 (0.00-0.00)	0.00 (0.00-0.00)	0.00 (0.00-0.00)	0.00 (0.00-0.00)

Values were median scores with (Minimum and Maximum values) and were based on scores ranging from 0 (absent) to 1 (present). All parameters listed were part of the 59-parameter dataset. [a]$p < 0.05$ with comparisons made between Clusters 2 and 3 or Clusters 5 and 6 or Clusters 7 and 8.

Table 6. Parameter Scores for Glomeruli Evaluated by Immunofluorescence Microscopy

PATTERN OR INJURY	Cluster 1 (Control)	Cluster 2 (FSGS)	Cluster 3 (FSGS)	Cluster 4 (Amyloidosis)	Cluster 5 (MPGN)	Cluster 6 (MPGN)	Cluster 7 (MGN)	Cluster 8 (MGN)
IgG mesangium	0.0 (0.0-1.0)	1.0 (0.0-2.0)	0.0 (0.0-1.0)	0.0 (0.0-1.0)	1.0 (0.0-2.0)	2.0 (0.0-2.0)	1.0 (0.0-2.0)	0.5 (0.0-2.0)
IgG capillary wall	0.0 (0.0-0.0)	0.0 (0.0-2.0)	0.0 (0.0-1.0)	0.0 (0.0-1.0)	2.0 (0.0-2.0)	2.0 (1.0-2.0)	2.0 (1.0-2.0)	2.0 (1.0-2.0)
IgM mesangium	1.0 (1.0-2.0)	2.0 (0.0-2.0)	1.0 (0.0-2.0)	0.0 (0.0-2.0)	2.0 (0.0-2.0)	2.0 (0.0-2.0)	1.0 (0.0-2.0)	1.5 (0.0-2.0)
IgM capillary wall	0.0 (0.0-2.0)	1.0[a] (0.0-2.0)	0.0 (0.0-1.0)	0.0 (0.0-1.0)	1.5 (0.0-2.0)	2.0 (0.0-2.0)	1.0 (0.0-2.0)	1.5 (0.0-2.0)
IgA mesangium	0.0 (0.0-0.0)	0.0 (0.0-2.0)	0.0 (0.0-1.0)	0.0 (0.0-1.0)	0.0 (0.0-1.0)	0.0 (0.0-1.0)	0.0 (0.0-2.0)	0.0 (0.0-2.0)
IgA capillary wall	0.0 (0.0-0.0)	0.0 (0.0-2.0)	0.0 (0.0-1.0)	0.0 (0.0-1.0)	0.0 (0.0-1.0)	0.0 (0.0-1.0)	0.0 (0.0-2.0)	0.0 (0.0-2.0)
C3 mesangium	0.0 (0.0-1.0)	0.0 (0.0-2.0)	0.0 (0.0-2.0)	0.0 (0.0-2.0)	2.0 (0.0-2.0)	2.0 (0.0-2.0)	2.0 (0.0-2.0)	1.0 (0.0-2.0)
C3 capillary wall	0.0 (0.0-0.0)	0.0 (0.0-2.0)	0.0 (0.0-2.0)	0.0 (0.0-1.0)	2.0 (0.0-2.0)	2.0 (1.0-2.0)	2.0 (1.0-2.0)	2.0 (0.0-2.0)

Values were median scores with (Minimum and Maximum values) and were based on the absence or presence of a fluorescent granular pattern ranging from 0-2 (0, absent; 1, equivocal; 2, present). All parameters listed were part of the 59-parameter dataset. [a]$p < 0.05$ with comparisons made between Cluster 2 and 3, Cluster 5 and 6, and Cluster 7 and 8.

Table 7. Summary of clinical data

CLINICAL VARIABLE	Cluster 1 Control n=5	Cluster 2 (FSGS) n=13	Cluster 3 (FSGS) n=13	Cluster 4 (Amyloidosis) n=12	Cluster 5 (MPGN) n=10	Cluster 6 (MPGN) n=13	Cluster 7 (MGN) n=13	Cluster 8 (MGN) n=10
UPC								
Median	0.13	5.6	8.7	9.8	16.1	9.6	8.9	16.0
Min - Max	0.05 – 0.25	2.6 - 26.3	5.1 – 24.5	6.2 – 26.1	6.9 – 23.6	3.7 – 30.1	3.4 – 21.9	4.2 – 42.7
SCr (mg/dL)								
Median	1.6	1.1	1.3	1.2	3.6	1.6	1.1	1.0
Min - Max	1.1 – 1.8	0.5 – 4.8	0.5 – 4.2	0.6 – 8.6	1.0 – 5.7	0.7 – 3.6	0.8 – 3.7	0.6 – 4.2
SAlb (g/dL)								
Median	3.8	2.3	2.4	1.8	1.4	1.6	1.6	1.6
Min - Max	3.6 – 4.4	1.3 – 3.8	1.5 – 4.1	0.9 – 2.4	1.0 – 1.9	1.1 – 3.1	1.1 – 3.1	0.7 – 2.7
Hypertension[1]								
No. hypertensive	4 of 5	5 of 13	9 of 13	3 of 11	9 of 10	10 of 12	4 of 10	6 of 8

All control dogs were female greyhounds. [1]Hypertension as defined in the text. UPC: urine protein:creatinine ratio (reference interval, <0.5), SCr: serum creatinine concentration (reference interval, 0.5-1.5mg/dL), SAlb: serum albumin concentration (reference interval, 2.5-4.0g/dL).

Figure 1. Dendrogram of 89 patients based on cluster analysis evaluation of 114 parameters related to all compartments of the kidney. Evaluation was performed by light microscopy, transmission electron microscopy, and immunofluorescence microscopy. The numbered (1–8) horizontal bar shows the level of discrimination that delineates the 8 clusters identified. Cluster 1 was composed of 5 control animals with normal glomerular morphology, clinical findings, and laboratory values. Clusters 2 and 3 comprised cases with glomerulosclerosis. Interestingly, cases in cluster 2 shared more similarities to controls in cluster 1 than to cases in cluster 3, as demonstrated by the presence of a connecting link between clusters 1 and 2. Cluster 4 comprised cases of glomerular amyloidosis. Cases in clusters 5 and 6 and clusters 7 and 8 had patterns that were characteristic of membranoproliferative glomerulonephritis and membranous glomerulonephropathy, respectively.

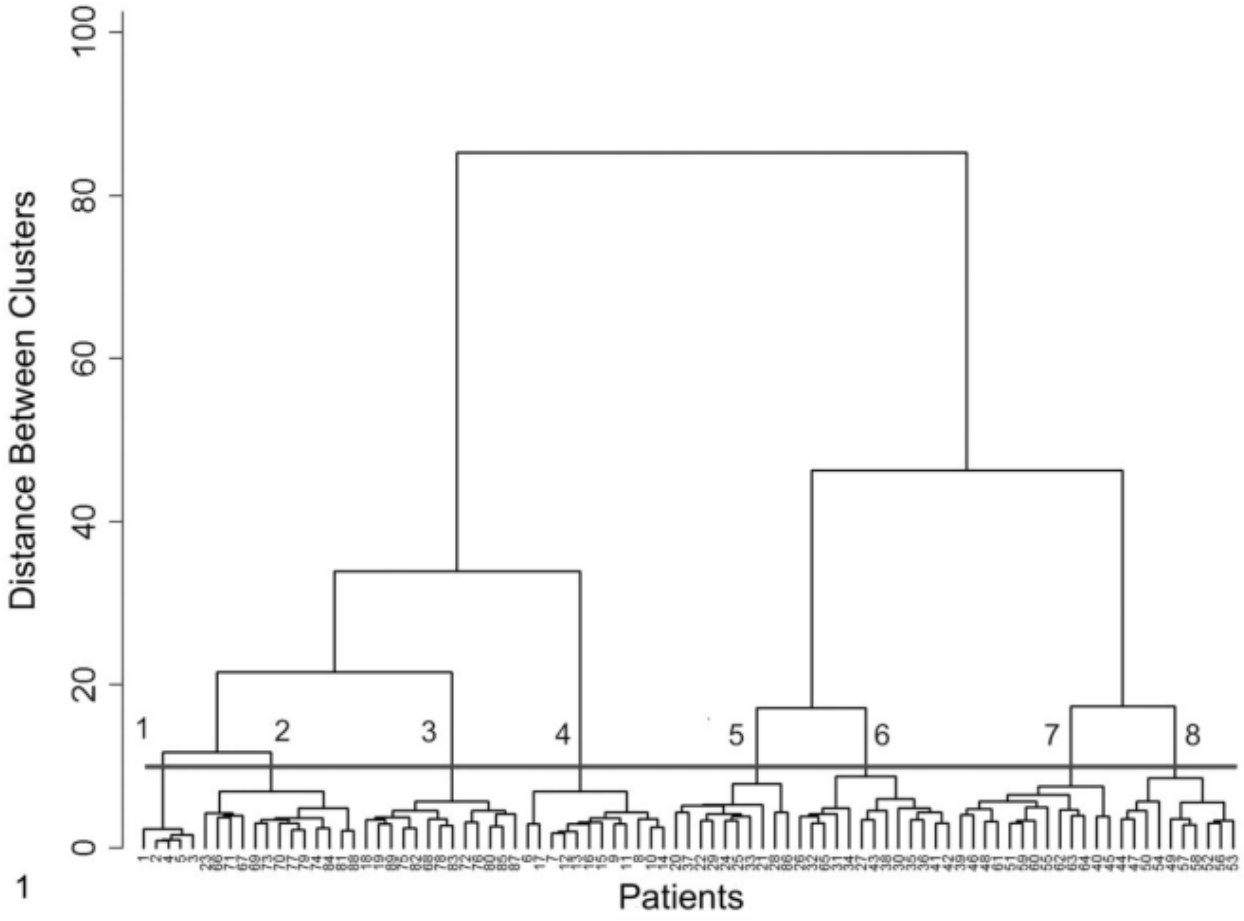

Figure 2. Dendrogram of 89 patients based on cluster analysis of 59 parameters related to all compartments of the kidney and evaluated by light microscopy, transmission electron microscopy, and immunofluorescence microscopy. The numbered (1–8) horizontal bar shows the level of discrimination that delineates the 8 clusters identified. The star indicates a case that moved from cluster 6 in the 114-parameter dendrogram to cluster 7 in the 59-parameter dendrogram.

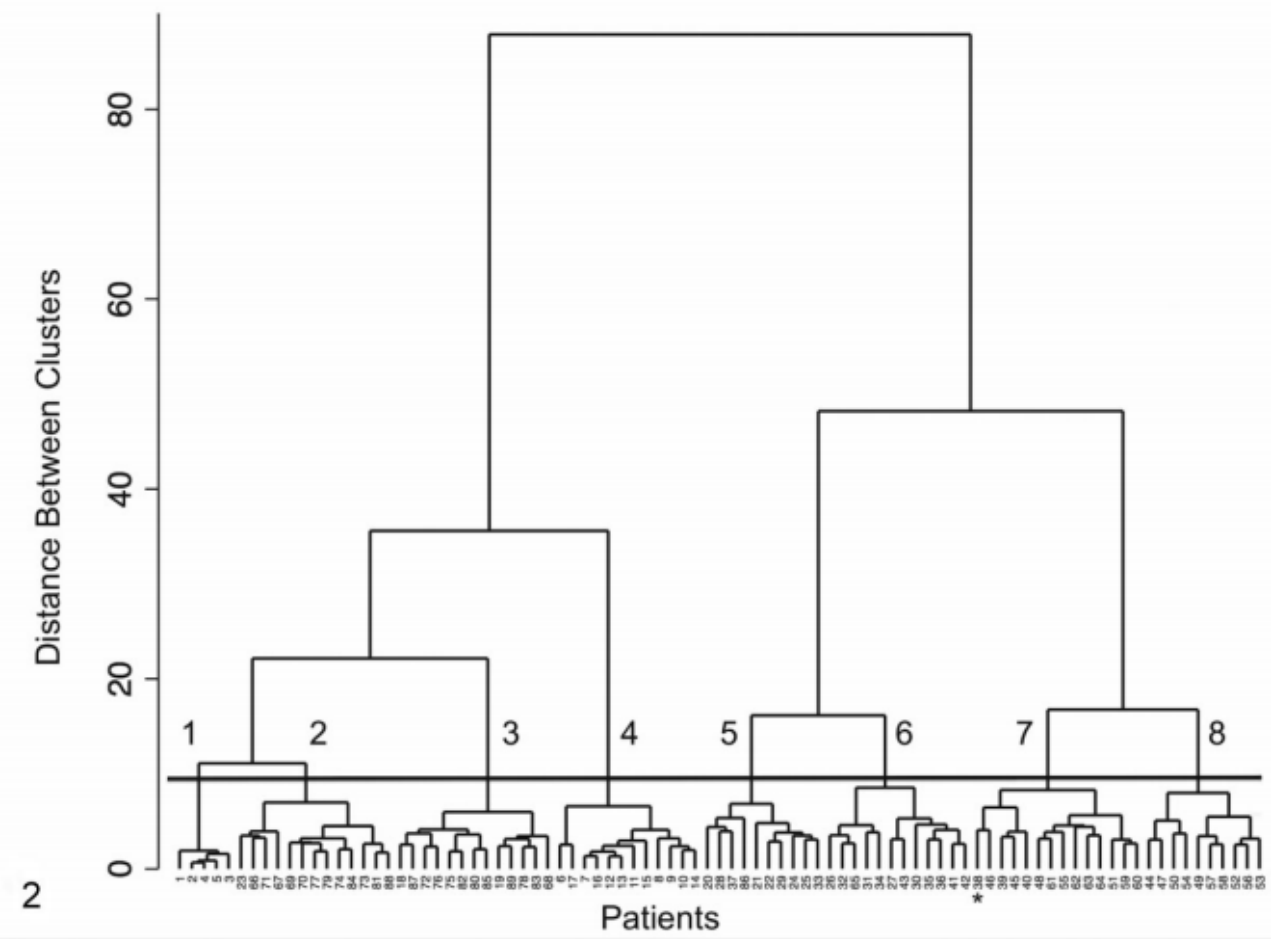

Figure 3. Evaluation of 35 light microscopic parameters derived from the 59-parameter data set. The numbered (1–8) horizontal bar shows the level of discrimination that delineates the 8 clusters identified. Ovals indicate cases that moved from clusters 7 and 8 of the 59-parameter data set (represented by Fig. 2) to clusters 2 and 3 of the 35-parameter data set. Rectangles indicate cases that moved from clusters 2 and 3 of the 59-parameter data set to cluster 5 of the 35-parameter data set.

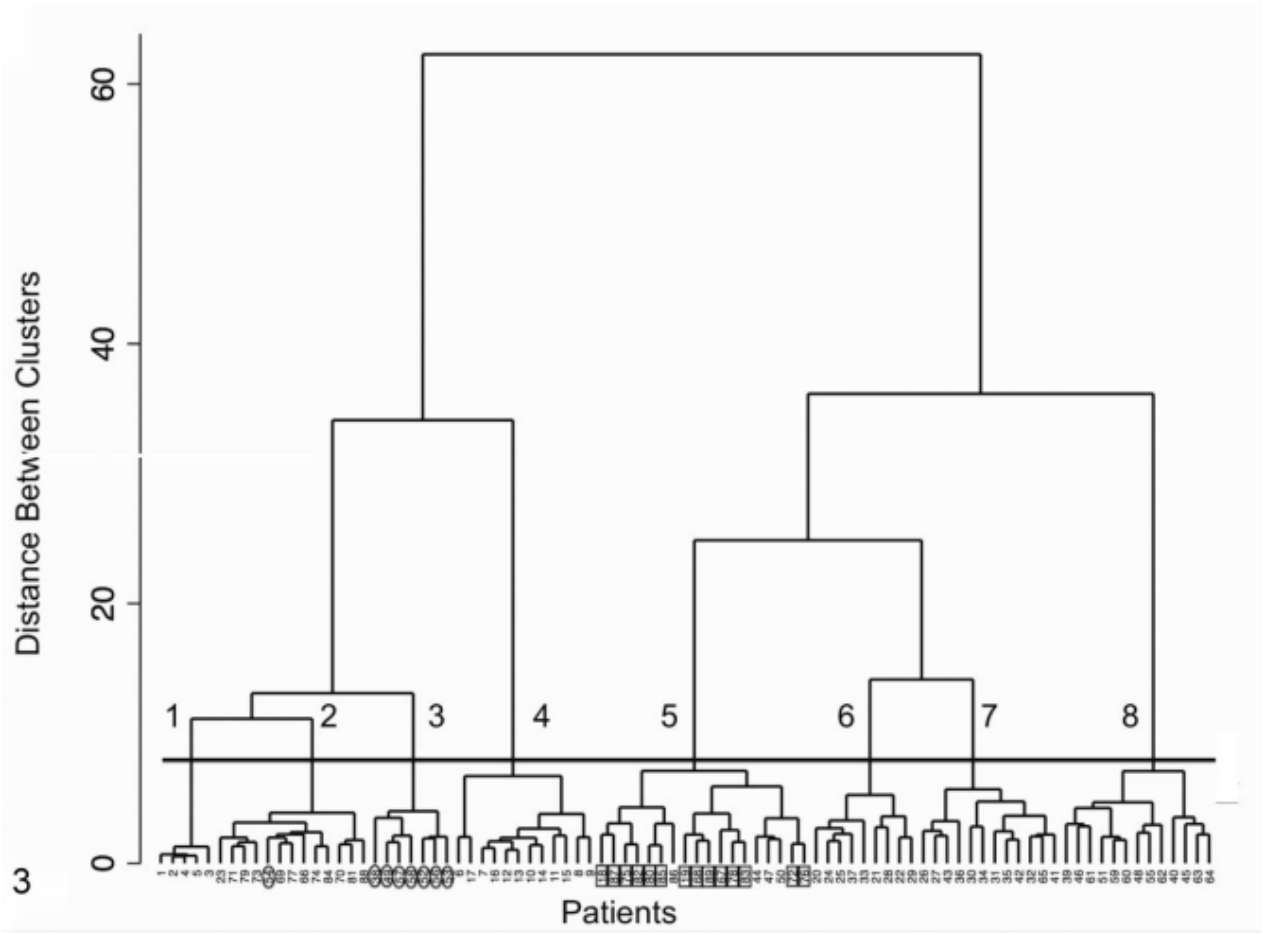

Figures 4–9. Normal glomerulus, control dog, cluster 1. Figures 4–7. The glomerulus is normocellular; mesangium is not expanded; and the glomerular basement membrane is of normal thickness with a smooth outer contour. There is mild thickening and splitting of the basement membrane of Bowman capsule. Figure 4. Hematoxylin and eosin. Figure 5. Periodic acid–Schiff reaction. Figure 6. Masson trichrome. Figure 7. Jones methenamine silver. Figure 8. Normal glomerular capillary loops from the same dog. Capillary lumens are open, and endothelial cells are at the base of the capillary loops. Podocyte foot processes are perpendicularly oriented along the capillary walls. One capillary loop in upper-right corner has subendothelial widening. Bar ¼ 2 mm. Transmission electron microscopy. Figure 9. Immunofluorescence for IgM shows scattered, equivocal staining at the periphery of the tuft

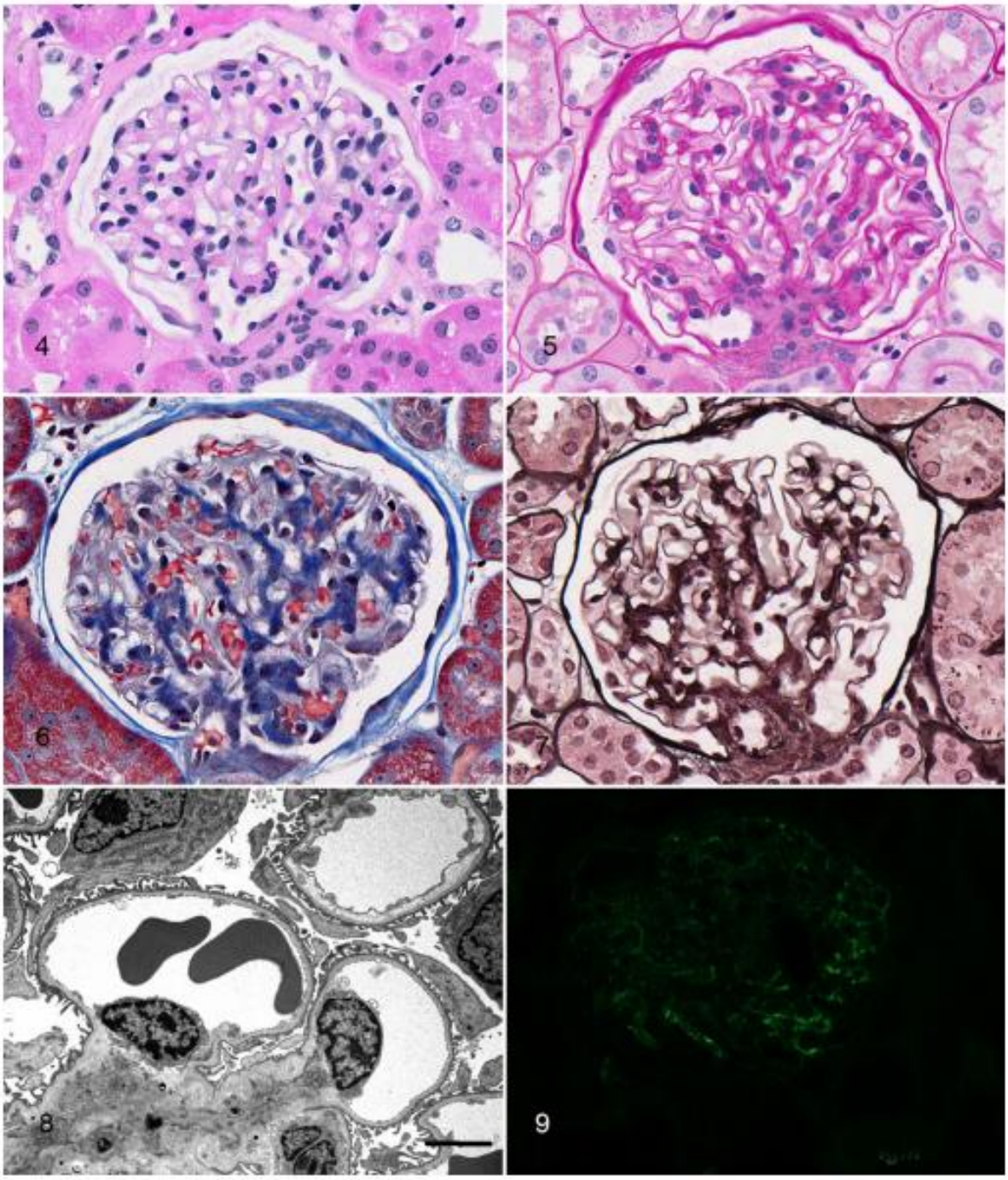

Figures 10–15. Focal segmental glomerulosclerosis, dog, cluster 3. Figures 10–13. There is segmental consolidation of capillary lumens by extracellular matrix and multiple synechiae (arrows). Some parietal epithelium and podocytes are hypertrophied. Figure 10. Hematoxylin and eosin. Figure 11. Periodic acid–Schiff reaction. Figure 12. There is moderate periglomerular fibrosis (*). Masson trichrome. Figure 13. Jones methenamine silver. Figure 14. Glomerulus from the same dog. There is global effacement of podocyte foot processes (arrowheads) and swelling of podocyte cytoplasm such that the urinary space cannot be identified. Bar ¼ 2 mm. Transmission electron microscopy. Figure 15. Immunofluorescence for IgG is negative.

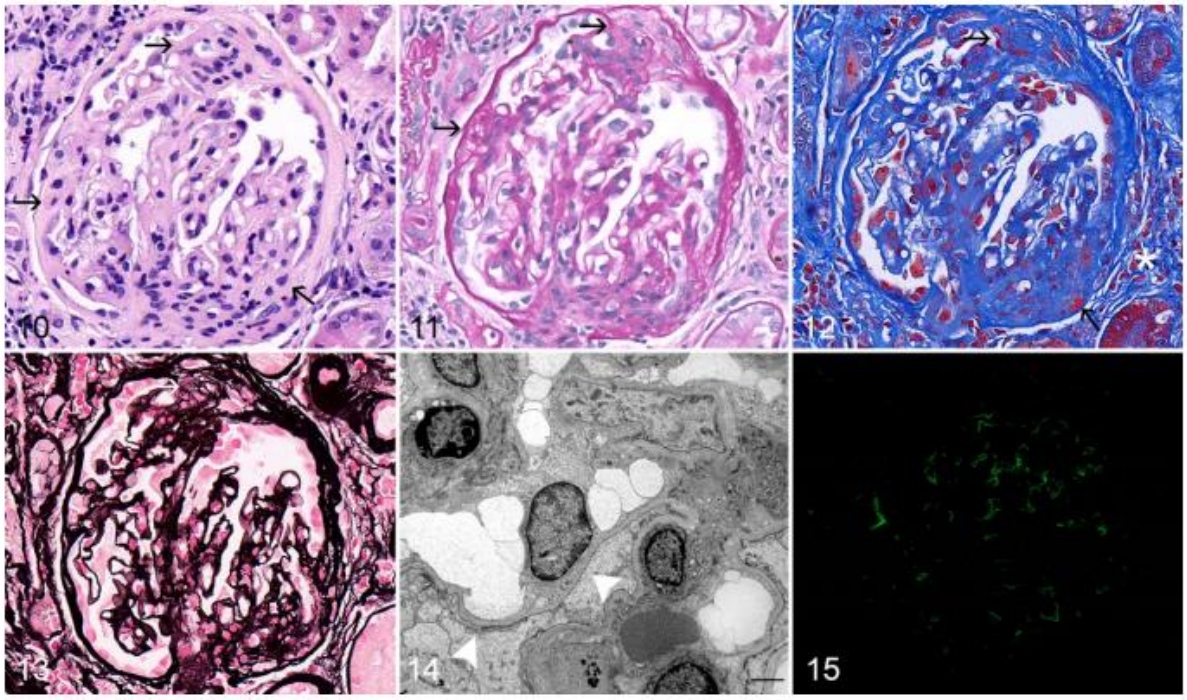

Figures 16–23. Glomerular amyloidosis, dog, cluster 4. Figure 16. There is expansion of the mesangium by eosinophilic material. Hematoxylin and eosin. Figure 17. The material appears waxy pink. Periodic acid–Schiff reaction. Figure 18. The material is mottled blue to peach. Masson trichrome. Figure 19. The material does not take up silver. Jones methenamine silver. Figure 20. The material is congophilic. Congo red. Figure 21. The material demonstrates apple green birefringence. Congo red viewed with polarized light. Figure 22. Glomerulus from the same dog. The mesangium is expanded by amorphous electron-dense material (*). Bar ¼ 5 mm. Transmission electron microscopy. Figure 23. Higher magnification of the same glomerulus demonstrates amyloid fibrils organized into spikelike projections along capillary wall. There is podocyte foot process effacement. Bar ¼ 1 mm. Transmission electron microscopy

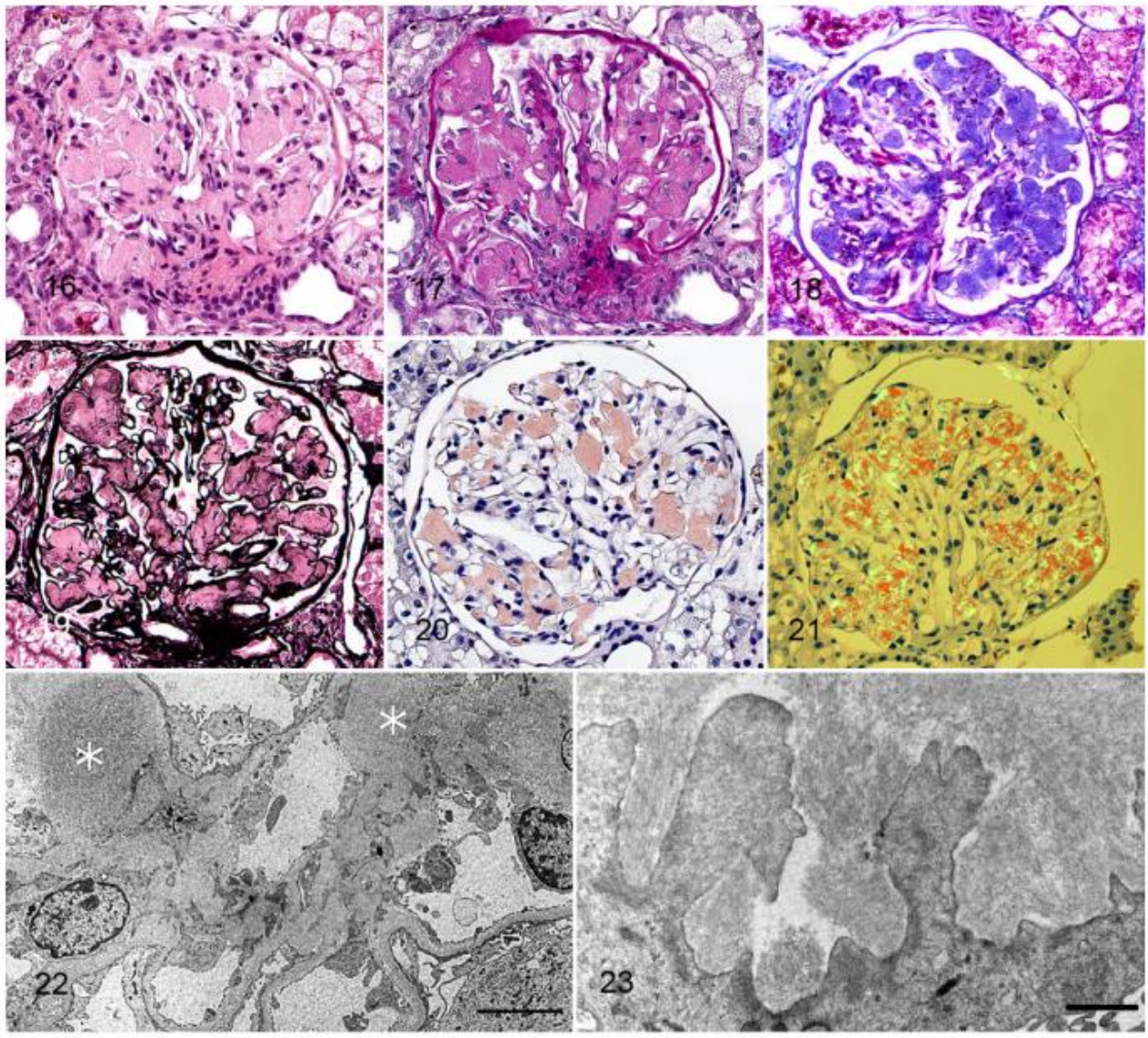

Figures 24–29. Membranoproliferative glomerulonephritis, dog, cluster 5. Figures 24, 25. There are global mesangial hypercellularity and segmental endocapillary hypercellularity. Capillary lumens are compressed by the expanded mesangium, thickened glomerular basement membrane (GBM), swollen endothelial cells, and interposed mesangial cells. Figure 24. Hematoxylin and eosin. Figure 25. Periodic acid–Schiff reaction. Figure 26. There is peach to orange material in the mesangium and capillary walls (hyalinosis). Masson trichrome. Figure 27. There are double contours of the GBM. Small synechiae are present. Jones methenamine silver. Figure 28. Glomerulus from the same dog. The GBM is thickened due to the presence of variably electron-dense deposits in a subendothelial location. There is endothelial swelling and podocyte foot process effacement. Bar ¼ 2 mm. Transmission electron microscopy. Figure 29. Immunofluorescence for IgG shows unequivocal granular staining along capillary loops and mesangium.

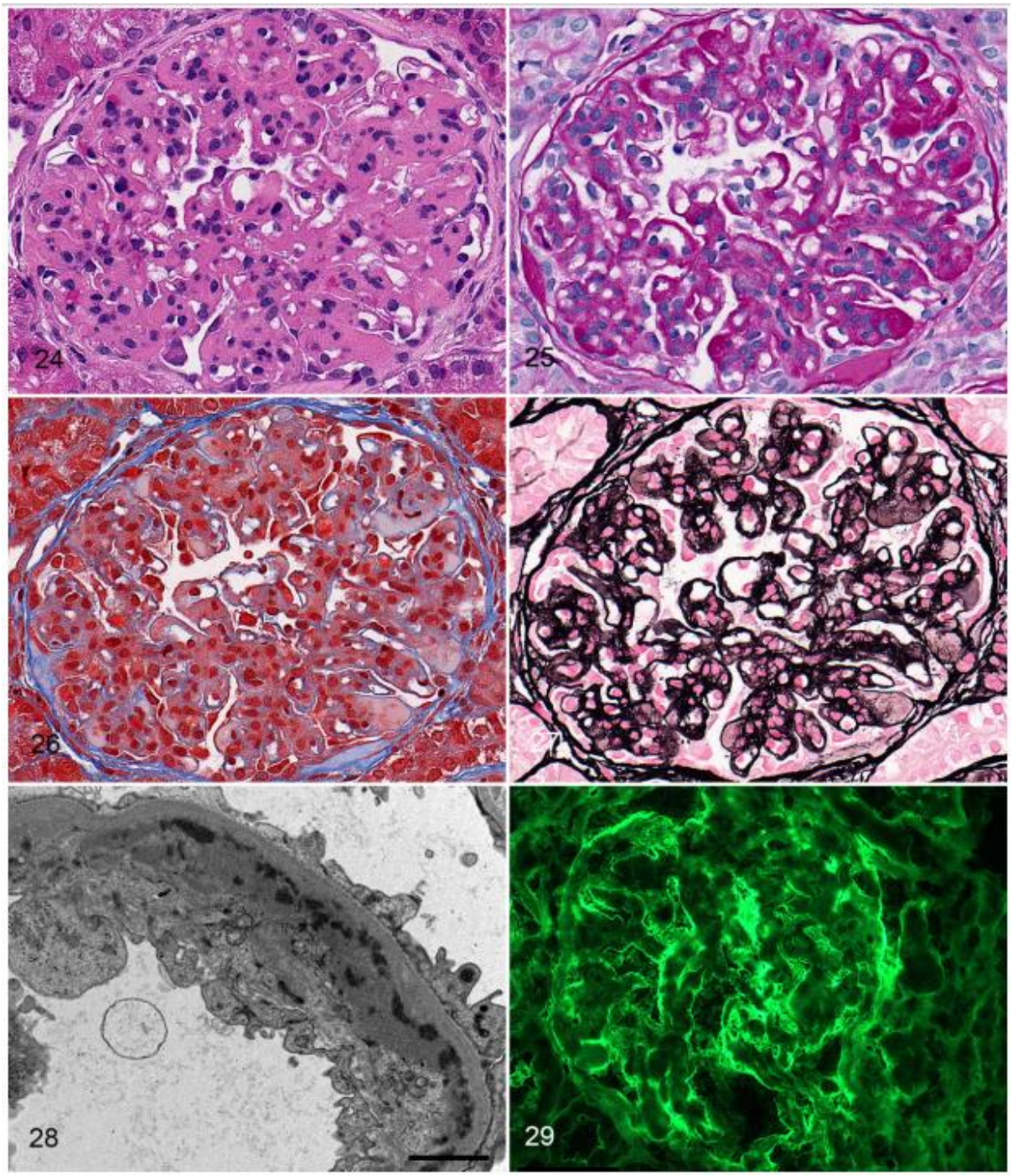

Figures 30–35. Membranous glomerulonephropathy, dog, cluster 7. Figures 30, 31. There is mild segmental mesangial hypercellularity and moderate thickening of the capillary walls. Podocytes are markedly hypertrophied. Figure 30. Hematoxylin and eosin. Figure 31. Periodic acid–Schiff reaction. Figure 32. There are regularly spaced red nodules along the abluminal surface of the capillary walls, consistent with immune deposits (arrows). Masson trichrome. Figure 33. There are ‘‘spikes’’ and ‘‘holes’’ along the abluminal surface. Jones methenamine silver. Figure 34. Glomerulus from the same dog. There are numerous electron dense deposits (*) on the abluminal surface of the capillary wall, some of which have a moth-eaten appearance indicative of dissolution. Deposits are separated by spikes (arrows) or encircled by the glomerular basement membrane (arrowhead). Podocyte foot processes are globally effaced, and microvillus transformation of podocyte cytoplasm is prominent. Bar¼ 2 mm. Transmission electron microscopy.Figure 35. Immunofluorescence for IgG shows unequivocal granular staining along capillary loops.